[70] Li X, Okada Y, Pilbeam CC, Lorenzo JA, Kennedy CR, Breyer RM, et al. Knockout of the murine prostaglandin $EP_2$ receptor impairs osteoclastogenesis in vitro. Endocrinology 2000;141: 2054–61.

[71] Alander CB, Raisz LG. Effects of selective prostaglandins $E_2$ receptor agonists on cultured calvarial murine osteoblastic cells. Prostaglandins Other Lipid Mediat 2006;81:178–83.

[72] Suda M, Tanaka K, Yasoda A, Natsui K, Sakuma Y, Tanaka I, et al. Prostaglandin $E_2$ ($PGE_2$) autoamplifies its production through $EP_1$ subtype of PGE receptor in mouse osteoblastic MC3T3-E1 cells. Calcif Tissue Int 1998;62:327–31.

[73] Fujieda M, Kiriu M, Mizuochi S, Hagiya K, Kaneki H, Ide H. Formation of mineralized bone nodules by rat calvarial osteoblasts decreases with donor age due to a reduction in signaling through $EP_1$ subtype of prostaglandin $E_2$ receptor. J Cell Biochem 1999;75:215–25.

[74] Tang CH, Yang RS, Fu WM. Prostaglandin $E_2$ stimulates fibronectin expression through $EP_1$ receptor, phospholipase C, protein kinase Cα, and c-Src pathway in primary cultured rat osteoblasts. J Biol Chem 2005;280:22907–16.

[75] Udagawa N, Takahashi N, Jimi E, Matsuzaki K, Tsurukai T, Itoh K, et al. Osteoblasts/stromal cells stimulate osteoclast activation through expression of osteoclast differentiation factor/RANKL but not macrophage colony-stimulating factor. Bone 1999;25:517–23.

[76] Yasuda H, Shima N, Nakagawa N, Yamaguchi K, Kinosaki M, Mochizuki S, et al. Osteoclast differentiation factor is a ligand for osteoprotegerin/osteoclastogenesis-inhibitory factor and is identical to TRANCE/RANKL. Proc Natl Acad Sci USA 1998;95:3597–602.

[77] Fuller K, Wong B, Fox S, Choi Y, Chambers TJ. TRANCE is necessary and sufficient for osteoblast-mediated activation of bone resorption in osteoclasts. J Exp Med 1998;188:997–1001.

[78] Simonet WS, Lacey DL, Dunstan CR, Kelley M, Chang MS, Luthy R, et al. Osteoprotegerin: a novel secreted protein involved in the regulation of bone density. Cell 1997;89:309–19.

[79] Brandstrom H, Jonsson KB, Ohlsson C, Vidal O, Ljunghall S, Ljunggren O. Regulation of osteoprotegerin mRNA levels by prostaglandin $E_2$ in human bone marrow stroma cells. Biochem Biophys Res Commun 1998;247:338–41.

[80] Suda K, Udagawa N, Sato N, Takami M, Itoh K, Woo JT, et al. Suppression of osteoprotegerin expression by prostaglandin $E_2$ is crucially involved in lipopolysaccharide-induced osteoclast formation. J Immunol 2004;172:2504–10.

[81] Ishimi Y, Miyaura C, Jin CH, Akatsu T, Abe E, Nakamura Y, et al. IL-6 is produced by osteoblasts and induces bone resorption. J Immunol 1990;145:3297–303.

[82] Devlin RD, Reddy SV, Savino R, Ciliberto G, Roodman GD. IL-6 mediates the effects of IL-1 or TNF, but not PTHrP or $1,25(OH)_2D_3$, on osteoclast-like cell formation in normal human bone marrow cultures. J Bone Miner Res 1998;13:393–9.

[83] Kozawa O, Suzuki A, Tokuda H, Kaida T, Uematsu T. Interleukin-6 synthesis induced by prostaglandin $E_2$: cross-talk regulation by protein kinase C. Bone 1998;22:355–60.

[84] Gruber R, Nothegger G, Ho GM, Willheim M, Peterlik M. Differential stimulation by $PGE_2$ and calcemic hormones of IL-6 in stromal/osteoblastic cells. Biochem Biophys Res Commun 2000;270:1080–5.

[85] Millet I, McCarthy TL, Vignery A. Regulation of interleukin-6 production by prostaglandin $E_2$ in fetal rat osteoblasts: role of protein kinase A signaling pathway. J Bone Miner Res 1998;13:1092–100.

[86] Taga T, Hibi M, Hirata Y, Yamasaki K, Yasukawa K, Matsuda T, et al. Interleukin-6 triggers the association of its receptor with a possible signal transducer, gp130. Cell 1989;58:573–81.

[87] Udagawa N, Takahashi N, Katagiri T, Tamura T, Wada S, Findlay DM, et al. Interleukin (IL)-6 induction of osteoclast differentiation depends on IL-6 receptors expressed on osteoblastic cells but not on osteoclast progenitors. J Exp Med 1995;182:1461–8.

[88] Palmqvist P, Persson E, Conaway HH, Lerner UH. IL-6, leukemia inhibitory factor, and oncostatin M stimulate bone resorption and regulate the expression of receptor activator of NF-κB ligand, osteoprotegerin, and receptor activator of NF-κB in mouse calvariae. J Immunol 2002;169:3353–62.

[89] Honda M, Yamamoto S, Cheng M, Yasukawa K, Suzuki H, Saito T, et al. Human soluble IL-6 receptor: its detection and enhanced release by HIV infection. J Immunol 1992;148: 2175–80.

[90] Liu XH, Kirschenbaum A, Yao S, Levine AC. Cross-talk between the interleukin-6 and prostaglandin $E_2$ signaling systems results in enhancement of osteoclastogenesis through effects on the osteoprotegerin/receptor activator of nuclear factor-κB (RANK) ligand/RANK system. Endocrinology 2005;146:1991–8.

[91] Lorenzo JA, Sousa SL, Alander C, Raisz LG, Dinarello CA. Comparison of the bone-resorbing activity in the supernatants from phytohemagglutinin-stimulated human peripheral blood mononuclear cells with that of cytokines through the use of an antiserum to interleukin 1. Endocrinology 1987;121:1164–70.

[92] Linkhart TA, MacCharles DC. Interleukin-1 stimulates release of insulin-like growth factor-I from neonatal mouse calvaria by a prostaglandin synthesis-dependent mechanism. Endocrinology 1992;131:2297–305.

[93] Amano S, Naganuma K, Kawata Y, Kawakami K, Kitano S, Hanazawa S. Prostaglandin $E_2$ stimulates osteoclast formation via endogenous IL-1β expressed through protein kinase A. J Immunol 1996;156:1931–6.

[94] Park YG, Kang SK, Noh SH, Park KK, Chang YC, Lee YC, et al. $PGE_2$ induces IL-1β gene expression in mouse osteoblasts through a cAMP-PKA signaling pathway. Int Immunopharmacol 2004;4:779–89.

[95] Akatsu T, Takahashi N, Udagawa N, Imamura K, Yamaguchi A, Sato K, et al. Role of prostaglandins in interleukin-1-induced bone resorption in mice in vitro. J Bone Miner Res 1991;6:183–9.

[96] Tanabe N, Maeno M, Suzuki N, Fujisaki K, Tanaka H, Ogiso B, et al. IL-1α stimulates the formation of osteoclast-like cells by increasing M-CSF and $PGE_2$ production and decreasing OPG production by osteoblasts. Life Sci 2005;77:615–26.

[97] Jimi E, Ikebe T, Takahashi N, Hirata M, Suda T, Koga T. Interleukin-1α activates an NF-κB-like factor in osteoclast-like cells. J Biol Chem 1996;271:4605–8.

[98] Jimi E, Nakamura I, Ikebe T, Akiyama S, Takahashi N, Suda T. Activation of NF-κB is involved in the survival of osteoclasts promoted by interleukin-1. J Biol Chem 1998;273:8799–805.

[99] Pilbeam CC, Raisz LG, Voznesensky O, Alander CB, Delman BN, Kawaguchi H. Autoregulation of inducible prostaglandin G/H synthase in osteoblastic cells by prostaglandins. J Bone Miner Res 1995;10:406–14.

[100] Murakami M, Kuwata H, Amakasu Y, Shimbara S, Nakatani Y, Atsumi G, et al. Prostaglandin $E_2$ amplifies cytosolic phospholipase $A_2$- and cyclooxygenase-2-dependent delayed prostaglandin $E_2$ generation in mouse osteoblastic cells. Enhancement by secretory phospholipase $A_2$. J Biol Chem 1997;272:19891–7.

[101] Chambers TJ, Thomson BM, Fuller K. Effect of substrate composition on bone resorption by rabbit osteoclasts. J Cell Sci 1984;70:61–71.

[102] Sakamoto S, Sakamoto M. Osteoblast collagenase: collagenase synthesis by clonally derived mouse osteogenic (MC3T3-E1) cells. Biochem Int 1984;9:51–8.

[103] Holliday LS, Welgus HG, Fliszar CJ, Veith GM, Jeffrey JJ, Gluck SL. Initiation of osteoclast bone resorption by interstitial collagenase. J Biol Chem 1997;272:22053–8.

[104] Kim CH, Park YG, Noh SH, Kim YK. $PGE_2$ induces the gene expression of bone matrix metalloproteinase-1 in mouse osteoblasts by cAMP-PKA signaling pathway. Int J Biochem Cell Biol 2005;37:375–85.

[105] Blobel CP. Metalloprotease-disintegrins: links to cell adhesion and cleavage of TNFα and Notch. Cell 1997;90:589–92.

[106] Miles RR, Sluka JP, Halladay DL, Santerre RF, Hale LV, Bloem L, et al. ADAMTS-1: a cellular disintegrin and metalloprotease with thrombospondin motifs is a target for parathyroid hormone in bone. Endocrinology 2000;141:4533–42.
[107] Komori T. Requisite roles of Runx2 and Cbfb in skeletal development. J Bone Miner Metab 2003;21:193–7.
[108] Yoshida K, Oida H, Kobayashi T, Maruyama T, Tanaka M, Katayama T, et al. Stimulation of bone formation and prevention of bone loss by prostaglandin E EP4 receptor activation. Proc Natl Acad Sci USA 2002;99:4580–5.
[109] Wozney JM, Rosen V. Bone morphogenetic protein and bone morphogenetic protein gene family in bone formation and repair. Clin Orthop Relat Res 1998:26–37.
[110] Ducy P, Zhang R, Geoffroy V, Ridall AL, Karsenty G. Osf2/Cbfa1: a transcriptional activator of osteoblast differentiation. Cell 1997;89:747–54.
[111] Arikawa T, Omura K, Morita I. Regulation of bone morphogenetic protein-2 expression by endogenous prostaglandin $E_2$ in human mesenchymal stem cells. J Cell Physiol 2004;200:400–6.
[112] Garcia AJ, Reyes CD. Bio-adhesive surfaces to promote osteoblast differentiation and bone formation. J Dent Res 2005;84:407–13.
[113] Hakeda Y, Nakatani Y, Kurihara N, Ikeda E, Maeda N, Kumegawa M. Prostaglandin $E_2$ stimulates collagen and non-collagen protein synthesis and prolyl hydroxylase activity in osteoblastic clone MC3T3-E1 cells. Biochem Biophys Res Commun 1985;126:340–5.
[114] Globus RK, Doty SB, Lull JC, Holmuhamedov E, Humphries MJ, Damsky CH. Fibronectin is a survival factor for differentiated osteoblasts. J Cell Sci 1998;111:1385–93.
[115] Samoto H, Shimizu E, Matsuda-Honjyo Y, Saito R, Nakao S, Yamazaki M, et al. Prostaglandin $E_2$ stimulates bone sialoprotein (BSP) expression through cAMP and fibroblast growth factor 2 response elements in the proximal promoter of the rat BSP gene. J Biol Chem 2003;278:28659–67.
[116] Wani MR, Fuller K, Kim NS, Choi Y, Chambers T. Prostaglandin $E_2$ cooperates with TRANCE in osteoclast induction from hemopoietic precursors: synergistic activation of differentiation, cell spreading, and fusion. Endocrinology 1999;140:1927–35.
[117] Kobayashi Y, Take I, Yamashita T, Mizoguchi T, Ninomiya T, Hattori T, et al. Prostaglandin $E_2$ receptors EP2 and EP4 are down-regulated during differentiation of mouse osteoclasts from their precursors. J Biol Chem 2005;280:24035–42.
[118] Kobayashi Y, Mizoguchi T, Take I, Kurihara S, Udagawa N, Takahashi N. Prostaglandin $E_2$ enhances osteoclastic differentiation of precursor cells through protein kinase A-dependent phosphorylation of TAK1. J Biol Chem 2005;280:11395–403.
[119] Take I, Kobayashi Y, Yamamoto Y, Tsuboi H, Ochi T, Uematsu S, et al. Prostaglandin $E_2$ strongly inhibits human osteoclast formation. Endocrinology 2005;146:5204–14.
[120] Lader CS, Flanagan AM. Prostaglandin $E_2$, interleukin 1α, and tumor necrosis factor-α increase human osteoclast formation and bone resorption in vitro. Endocrinology 1998;139:3157–64.
[121] Chenu C, Kurihara N, Mundy GR, Roodman GD. Prostaglandin $E_2$ inhibits formation of osteoclastlike cells in long-term human marrow cultures but is not a mediator of the inhibitory effects of transforming growth factor β. J Bone Miner Res 1990;5:677–81.
[122] Merke J, Klaus G, Hugel U, Waldherr R, Ritz E. No 1,25-dihydroxyvitamin $D_3$ receptors on osteoclasts of calcium-deficient chicken despite demonstrable receptors on circulating monocytes. J Clin Invest 1986;77:312–4.
[123] Kobayashi K, Takahashi N, Jimi E, Udagawa N, Takami M, Kotake S, et al. Tumor necrosis factor α stimulates osteoclast differentiation by a mechanism independent of the ODF/RANKL-RANK interaction. J Exp Med 2000;191:275–86.
[124] Itonaga I, Sabokbar A, Neale SD, Athanasou NA. 1,25-Dihydroxyvitamin $D_3$ and prostaglandin $E_2$ act directly on circulating human osteoclast precursors. Biochem Biophys Res Commun 1999;264:590–5.
[125] Suzuki H, Nakamura I, Takahashi N, Ikuhara T, Matsuzaki K, Isogai Y, et al. Calcitonin-induced changes in the cytoskeleton are mediated by a signal pathway associated with protein kinase A in osteoclasts. Endocrinology 1996;137:4685–90.
[126] Mano M, Arakawa T, Mano H, Nakagawa M, Kaneda T, Kaneko H, et al. Prostaglandin $E_2$ directly inhibits bone-resorbing activity of isolated mature osteoclasts mainly through the EP4 receptor. Calcif Tissue Int 2000;67:85–92.
[127] Sarrazin P, Hackett JA, Fortier I, Gallant MA, de Brum-Fernandes A. Role of EP3 and EP4 prostaglandin receptors in reorganization of the cytoskeleton in mature human osteoclasts. J Rheumatol 2004;31:1598–606.
[128] Li M, Healy DR, Li Y, Simmons HA, Crawford DT, Ke HZ, et al. Osteopenia and impaired fracture healing in aged EP4 receptor knockout mice. Bone 2005;37:46–54.
[129] Akhter MP, Cullen DM, Pan LC. Bone biomechanical properties in EP4 knockout mice. Calcif Tissue Int 2006;78:357–62.
[130] Akhter MP, Cullen DM, Gong G, Recker RR. Bone biomechanical properties in prostaglandin EP1 and EP2 knockout mice. Bone 2001;29:121–5.
[131] Lin BY, Jee WS, Ma YF, Ke HZ, Kimmel DB, Li XJ. Effects of prostaglandin $E_2$ and risedronate administration on cancellous bone in older female rats. Bone 1994;15:489–96.
[132] Suponitzky I, Weinreb M. Differential effects of systemic prostaglandin $E_2$ on bone mass in rat long bones and calvariae. J Endocrinol 1998;156:51–7.
[133] Li M, Ke HZ, Qi H, Healy DR, Li Y, Crawford DT, et al. A novel, non-prostanoid EP2 receptor-selective prostaglandin $E_2$ agonist stimulates local bone formation and enhances fracture healing. J Bone Miner Res 2003;18:2033–42.
[134] Bostrom MP. Expression of bone morphogenetic proteins in fracture healing. Clin Orthop Relat Res 1998:S116–23.
[135] Dekel S, Lenthall G, Francis MJ. Release of prostaglandins from bone and muscle after tibial fracture. An experimental study in rabbits. J Bone Joint Surg Br 1981;63-B:185–9.
[136] Gerstenfeld LC, Thiede M, Seibert K, Mielke C, Phippard D, Svagr B, et al. Differential inhibition of fracture healing by non-selective and cyclooxygenase-2 selective non-steroidal anti-inflammatory drugs. J Orthop Res 2003;21:670–5.
[137] Endo K, Sairyo K, Komatsubara S, Sasa T, Egawa H, Yonekura D, et al. Cyclooxygenase-2 inhibitor inhibits the fracture healing. J Physiol Anthropol Appl Human Sci 2002;21:235–8.
[138] Harder AT, An YH. The mechanisms of the inhibitory effects of nonsteroidal anti-inflammatory drugs on bone healing: a concise review. J Clin Pharmacol 2003;43:807–15.
[139] Zhang X, Schwarz EM, Young DA, Puzas JE, Rosier RN, O'Keefe RJ. Cyclooxygenase-2 regulates mesenchymal cell differentiation into the osteoblast lineage and is critically involved in bone repair. J Clin Invest 2002;109:1405–15.
[140] Paralkar VM, Borovecki F, Ke HZ, Cameron KO, Lefker B, Grasser WA, et al. An EP2 receptor-selective prostaglandin $E_2$ agonist induces bone healing. Proc Natl Acad Sci USA 2003;100:6736–40.
[141] Nomura S, Takano-Yamamoto T. Molecular events caused by mechanical stress in bone. Matrix Biol 2000;19:91–6.
[142] Stepan JJ, Pospichal J, Presl J, Pacovsky V. Bone loss and biochemical indices of bone remodeling in surgically induced postmenopausal women. Bone 1987;8:279–84.
[143] Ke HZ, Jee WS, Zeng QQ, Li M, Lin BY. Prostaglandin $E_2$ increased rat cortical bone mass when administered immediately following ovariectomy. Bone Miner 1993;21:189–201.
[144] Li M, Jee WS, Ke HZ, Tang LY, Ma YF, Liang XG, et al. Prostaglandin $E_2$ administration prevents bone loss induced by orchidectomy in rats. J Bone Miner Res 1995;10:66–73.

[145] Weinreb M, Grosskopf A, Shir N. The anabolic effect of $PGE_2$ in rat bone marrow cultures is mediated via the $EP_4$ receptor subtype. Am J Physiol 1999;276:E376–83.
[146] Ke HZ, Crawford DT, Qi H, Simmons HA, Owen TA, Paralkar VM, et al. A nonprostanoid EP4 receptor selective prostaglandin $E_2$ agonist restores bone mass and strength in aged, ovariectomized rats. J Bone Miner Res 2006;21:565–75.
[147] McClung MR. The menopause and HRT. Prevention and management of osteoporosis. Best Pract Res Clin Endocrinol Metab 2003;17:53–71.
[148] Lane N, Coble T, Kimmel DB. Effect of naproxen on cancellous bone in ovariectomized rats. J Bone Miner Res 1990;5:1029–35.
[149] Gregory LS, Kelly WL, Reid RC, Fairlie DP, Forwood MR. Inhibitors of cyclo-oxygenase-2 and secretory phospholipase $A_2$ preserve bone architecture following ovariectomy in adult rats. Bone 2006;39:134–42.
[150] Bauer DC, Orwoll ES, Fox KM, Vogt TM, Lane NE, Hochberg MC, et al. Aspirin and NSAID use in older women: effect on bone mineral density and fracture risk. Study of Osteoporotic Fractures Research Group. J Bone Miner Res 1996;11:29–35.
[151] Carbone LD, Tylavsky FA, Cauley JA, Harris TB, Lang TF, Bauer DC, et al. Association between bone mineral density and the use of nonsteroidal anti-inflammatory drugs and aspirin: impact of cyclooxygenase selectivity. J Bone Miner Res 2003;18:1795–802.
[152] Morton DJ, Barrett-Connor EL, Schneider DL. Nonsteroidal antiinflammatory drugs and bone mineral density in older women: the Rancho Bernardo study. J Bone Miner Res 1998;13:1924–31.
[153] Ono K, Akatsu T, Murakami T, Nishikawa M, Yamamoto M, Kugai N, et al. Important role of $EP_4$, a subtype of prostaglandin (PG) E receptor, in osteoclast-like cell formation from mouse bone marrow cells induced by $PGE_2$. J Endocrinol 1998;158:R1–5.
[154] Sato K, Takayanagi H. Osteoclasts, rheumatoid arthritis, and osteoimmunology. Curr Opin Rheumatol 2006;18:419–26.
[155] Martel-Pelletier J, Pelletier JP, Fahmi H. Cyclooxygenase-2 and prostaglandins in articular tissues. Semin Arthritis Rheum 2003;33:155–67.
[156] Kotake S, Udagawa N, Takahashi N, Matsuzaki K, Itoh K, Ishiyama S, et al. IL-17 in synovial fluids from patients with rheumatoid arthritis is a potent stimulator of osteoclastogenesis. J Clin Invest 1999;103:1345–52.
[157] Kojima F, Naraba H, Sasaki Y, Okamoto R, Koshino T, Kawai S. Coexpression of microsomal prostaglandin E synthase with cyclooxygenase-2 in human rheumatoid synovial cells. J Rheumatol 2002;29:1836–42.
[158] Korotkova M, Westman M, Gheorghe KR, af Klint E, Trollmo C, Ulfgren AK, et al. Effects of antirheumatic treatments on the prostaglandin $E_2$ biosynthetic pathway. Arthritis Rheum 2005;52:3439–47.
[159] Luross JA, Williams NA. The genetic and immunopathological processes underlying collagen-induced arthritis. Immunology 2001;103:407–16.
[160] Honda T, Segi-Nishida E, Miyachi Y, Narumiya S. Prostacyclin-IP signaling and prostaglandin $E_2$-EP2/EP4 signaling both mediate joint inflammation in mouse collagen-induced arthritis. J Exp Med 2006;203:325–35.
[161] Hegen M, Sun L, Uozumi N, Kume K, Goad ME, Nickerson-Nutter CL, et al. Cytosolic phospholipase $A_2\alpha$-deficient mice are resistant to collagen-induced arthritis. J Exp Med 2003;197:1297–302.
[162] Myers LK, Kang AH, Postlethwaite AE, Rosloniec EF, Morham SG, Shlopov BV, et al. The genetic ablation of cyclooxygenase 2 prevents the development of autoimmune arthritis. Arthritis Rheum 2000;43:2687–93.
[163] Trebino CE, Stock JL, Gibbons CP, Naiman BM, Wachtmann TS, Umland JP, et al. Impaired inflammatory and pain responses in mice lacking an inducible prostaglandin E synthase. Proc Natl Acad Sci USA 2003;100:9044–9.
[164] Kamei D, Yamakawa K, Takegoshi Y, Mikami-Nakanishi M, Nakatani Y, Oh-Ishi S, et al. Reduced pain hypersensitivity and inflammation in mice lacking microsomal prostaglandin E synthase-1. J Biol Chem 2004;279:33684–95.
[165] McCoy JM, Wicks JR, Audoly LP. The role of prostaglandin $E_2$ receptors in the pathogenesis of rheumatoid arthritis. J Clin Invest 2002;110:651–8.
[166] Ghosh P, Smith M. Osteoarthritis, genetic and molecular mechanisms. Biogerontology 2002;3:85–8.
[167] Smith MD, Triantafillou S, Parker A, Youssef PP, Coleman M. Synovial membrane inflammation and cytokine production in patients with early osteoarthritis. J Rheumatol 1997;24:365–71.
[168] Hardy MM, Seibert K, Manning PT, Currie MG, Woerner BM, Edwards D, et al. Cyclooxygenase 2-dependent prostaglandin $E_2$ modulates cartilage proteoglycan degradation in human osteoarthritis explants. Arthritis Rheum 2002;46:1789–803.
[169] Inoue H, Takamori M, Shimoyama Y, Ishibashi H, Yamamoto S, Koshihara Y. Regulation by $PGE_2$ of the production of interleukin-6, macrophage colony stimulating factor, and vascular endothelial growth factor in human synovial fibroblasts. Br J Pharmacol 2002;136:287–95.
[170] Hilal G, Massicotte F, Martel-Pelletier J, Fernandes JC, Pelletier JP, Lajeunesse D. Endogenous prostaglandin $E_2$ and insulin-like growth factor 1 can modulate the levels of parathyroid hormone receptor in human osteoarthritic osteoblasts. J Bone Miner Res 2001;16:713–21.
[171] Blanco FJ, Guitian R, Vazquez-Martul E, de Toro FJ, Galdo F. Osteoarthritis chondrocytes die by apoptosis. A possible pathway for osteoarthritis pathology. Arthritis Rheum 1998;41:284–9.
[172] Notoya K, Jovanovic DV, Reboul P, Martel-Pelletier J, Mineau F, Pelletier JP. The induction of cell death in human osteoarthritis chondrocytes by nitric oxide is related to the production of prostaglandin $E_2$ via the induction of cyclooxygenase-2. J Immunol 2000;165:3402–10.
[173] Heitz-Mayfield LJ. Disease progression: identification of high-risk groups and individuals for periodontitis. J Clin Periodontol 2005;32(Suppl. 6):196–209.
[174] Rams TE, Listgarten MA, Slots J. *Actinobacillus actinomycetemcomitans* and *Porphyromonas gingivalis* subgingival presence, species-specific serum immunoglobulin G antibody levels, and periodontitis disease recurrence. J Periodontal Res 2006;41:228–34.
[175] Wada N, Maeda H, Yoshimine Y, Akamine A. Lipopolysaccharide stimulates expression of osteoprotegerin and receptor activator of NF-kappa B ligand in periodontal ligament fibroblasts through the induction of interleukin-1 beta and tumor necrosis factor-alpha. Bone 2004;35:629–35.
[176] Yip KH, Zheng MH, Feng HT, Steer JH, Joyce DA, Xu J. Sesquiterpene lactone parthenolide blocks lipopolysaccharide-induced osteolysis through the suppression of NF-κB activity. J Bone Miner Res 2004;19:1905–16.
[177] Fukushima H, Jimi E, Okamoto F, Motokawa W, Okabe K. IL-1-induced receptor activator of NF-κB ligand in human periodontal ligament cells involves ERK-dependent $PGE_2$ production. Bone 2005;36:267–75.
[178] Miyauchi M, Takata T, Ito H, Ogawa I, Kobayashi J, Nikai H, et al. Immunohistochemical detection of prostaglandins $E_2$, $F_{2\alpha}$, and 6-keto-prostaglandin $F_{1\alpha}$ in experimentally induced periapical inflammatory lesions in rats. J Endod 1996;22:635–7.
[179] Tsai CC, Hong YC, Chen CC, Wu YM. Measurement of prostaglandin $E_2$ and leukotriene $B_4$ in the gingival crevicular fluid. J Dent 1998;26:97–103.
[180] Miyaura C, Inada M, Matsumoto C, Ohshiba T, Uozumi N, Shimizu T, et al. An essential role of cytosolic phospholipase $A_2\alpha$ in prostaglandin $E_2$-mediated bone resorption associated with inflammation. J Exp Med 2003;197:1303–10.
[181] Inada M, Matsumoto C, Uematsu S, Akira S, Miyaura C. Membrane-bound prostaglandin E synthase-1-mediated prostaglandin $E_2$ production by osteoblast plays a critical role in

lipopolysaccharide-induced bone loss associated with inflammation. J Immunol 2006;177:1879–85.
[182] Sakuma Y, Tanaka K, Suda M, Komatsu Y, Yasoda A, Miura M, et al. Impaired bone resorption by lipopolysaccharide in vivo in mice deficient in the prostaglandin E receptor EP4 subtype. Infect Immun 2000;68:6819–25.
[183] Williams RC, Jeffcoat MK, Kaplan ML, Goldhaber P, Johnson HG, Wechter WJ. Flurbiprofen: a potent inhibitor of alveolar bone resorption in beagles. Science 1985;227:640–2.
[184] Williams RC, Jeffcoat MK, Howell TH, Rolla A, Stubbs D, Teoh KW, et al. Altering the progression of human alveolar bone loss with the non-steroidal anti-inflammatory drug flurbiprofen. J Periodontol 1989;60:485–90.
[185] Ramirez-Yanez GO, Seymour GJ, Walsh LJ, Forwood MR, Symons AL. Prostaglandin $E_2$ enhances alveolar bone formation in the rat mandible. Bone 2004;35:1361–8.
[186] Ramirez-Yanez GO, Seymour GJ, Symons AL. Local application of prostaglandin $E_2$ reduces trap, calcitonin receptor and metalloproteinase-2 immunoreactivity in the rat periodontium. Arch Oral Biol 2005;50:1014–22.
[187] Feyen JH, van der Wilt G, Moonen P, Di Bon A, Nijweide PJ. Stimulation of arachidonic acid metabolism in primary cultures of osteoblast-like cells by hormones and drugs. Prostaglandins 1984;28:769–81.
[188] Cho MJ, Allen MA. Chemical stability of prostacyclin ($PGI_2$) in aqueous solutions. Prostaglandins 1978;15:943–54.
[189] Raisz LG, Vanderhoek JY, Simmons HA, Kream BE, Nicolaou KC. Prostaglandin synthesis by fetal rat bone in vitro: evidence for a role of prostacyclin. Prostaglandins 1979;17:905–14.
[190] Glanstchnig H, Varga F, Rumpler M, Klaushofer K. Prostacyclin ($PGI_2$): a potential mediator of c-fos expression induced by hydrostatic pressure in osteoblastic cells. Eur J Clin Invest 1996;26:544–8.
[191] Turner CH, Forwood MR, Rho JY, Yoshikawa T. Mechanical loading thresholds for lamellar and woven bone formation. J Bone Miner Res 1994;9:87–97.
[192] Joldersma M, Burger EH, Semeins CM, Klein-Nulend J. Mechanical stress induces COX-2 mRNA expression in bone cells from elderly women. J Biomech 2000;33:53–61.
[193] Chambers TJ, Fuller K, Athanasou NA. The effect of prostaglandins $I_2$, $E_1$, $E_2$ and dibutyryl cyclic AMP on the cytoplasmic spreading of rat osteoclasts. Br J Exp Pathol 1984;65:557–66.
[194] Maurin AC, Chavassieux PM, Meunier PJ. Expression of $PPAR_\gamma$ and β/δ in human primary osteoblastic cells: influence of polyunsaturated fatty acids. Calcif Tissue Int 2005;76:385–92.
[195] Brodie MJ, Hensby CN, Parke A, Gordon D. Is prostacyclin in the major pro-inflammatory prostanoid in joint fluid? Life Sci 1980;27:603–8.
[196] Tamura T, Udagawa N, Takahashi N, Miyaura C, Tanaka S, Yamada Y, et al. Soluble interleukin-6 receptor triggers osteoclast formation by interleukin 6. Proc Natl Acad Sci USA 1993;90:11924–8.
[197] Ishihara K, Hirano T. IL-6 in autoimmune disease and chronic inflammatory proliferative disease. Cytokine Growth Factor Rev 2002;13:357–68.
[198] Hakeda Y, Hotta T, Kurihara N, Ikeda E, Maeda N, Yagyu Y, et al. Prostaglandin $E_1$ and $F_{2\alpha}$ stimulate differentiation and proliferation, respectively, of clonal osteoblastic MC3T3-E1 cells by different second messengers in vitro. Endocrinology 1987;121:1966–74.
[199] Ma YF, Li XJ, Jee WS, McOsker J, Liang XG, Setterberg R, et al. Effects of prostaglandin $E_2$ and $F_{2\alpha}$ on the skeleton of osteopenic ovariectomized rats. Bone 1995;17:549–54.
[200] Tokuda H, Harada A, Hirade K, Matsuno H, Ito H, Kato K, et al. Incadronate amplifies prostaglandin $F_{2\alpha}$-induced vascular endothelial growth factor synthesis in osteoblasts. Enhancement of MAPK activity. J Biol Chem 2003;278:18930–7.
[201] Sabbieti MG, Marchetti L, Gabrielli MG, Menghi M, Materazzi S, Menghi G, et al. Prostaglandins differently regulate FGF-2 and FGF receptor expression and induce nuclear translocation in osteoblasts via MAPK kinase. Cell Tissue Res 2005;319:267–78.
[202] Harada S, Thomas KA. Vascular endothelial growth factors. In: Bilesikian JP, Raisz LG, Rodan GA, editors. Principles of bone biology. San Diego: Academic Press; 2002. p. 883–902.
[203] Hurley MM, Marie PJ, Florkiewicz RZ. Fibroblast growth factor (FGF) and FGF receptor families in bone. In: Bilesikian JP, Raisz LG, Rodan GA, editors. Principles of bone biology. San Diego: Academic Press; 2002. p. 825–52.
[204] Ahmed I, Gesty-Palmer D, Drezner MK, Luttrell LM. Transactivation of the epidermal growth factor receptor mediates parathyroid hormone and prostaglandin $F2_\alpha$-stimulated mitogen-activated protein kinase activation in cultured transgenic murine osteoblasts. Mol Endocrinol 2003;17:1607–21.
[205] Sato I, Suzuki A, Kakita A, Ono Y, Miura Y, Itoh M, et al. Stimulatory effect of prostaglandin $F_{2\alpha}$ on Na-dependent phosphate transport in osteoblast-like cells. Prostaglandins Leukot Essent Fatty Acids 2003;68:311–5.
[206] Koshihara Y, Kawamura M. Prostaglandin $D_2$ stimulates calcification of human osteoblastic cells. Biochem Biophys Res Commun 1989;159:1206–12.
[207] Tokuda H, Kozawa O, Harada A, Uematsu T. Prostaglandin $D_2$ induces interleukin-6 synthesis via $Ca^{2+}$ mobilization in osteoblasts: regulation by protein kinase C. Prostaglandins Leukot Essent Fatty Acids 1999;61:189–94.
[208] Takagi T, Yamamoto T, Asano S, Tamaki H. Effect of prostaglandin $D_2$ on the femoral bone mineral density in ovariectomized rats. Calcif Tissue Int 1993;52:442–6.
[209] Gallant MA, Samadfam R, Hackett JA, Antoniou J, Parent JL, de Brum-Fernandes AJ. Production of prostaglandin $D_2$ by human osteoblasts and modulation of osteoprotegerin, RANKL, and cellular migration by DP and CRTH2 receptors. J Bone Miner Res 2005;20:672–81.
[210] Siddhivarn C, Banes A, Champagne C, Riche EL, Weerapradist W, Offenbacher S. Prostaglandin $D_2$ pathway and peroxisome proliferator-activated receptor γ-1 expression are induced by mechanical loading in an osteoblastic cell line. J Periodontal Res 2006;41:92–100.
[211] Kakita A, Suzuki A, Ono Y, Miura Y, Itoh M, Oiso Y. Possible involvement of p38 MAP kinase in prostaglandin $E_1$-induced ALP activity in osteoblast-like cells. Prostaglandins Leukot Essent Fatty Acids 2004;70:469–74.
[212] Harada S, Nagy JA, Sullivan KA, Thomas KA, Endo N, Rodan GA, et al. Induction of vascular endothelial growth factor expression by prostaglandin $E_2$ and $E_1$ in osteoblasts. J Clin Invest 1994;93:2490–6.
[213] Kanno Y, Tokuda H, Nakajima K, Ishisaki A, Shibata T, Numata O, et al. Involvement of SAPK/JNK in prostaglandin $E_1$-induced VEGF synthesis in osteoblast-like cells. Mol Cell Endocrinol 2004;220:89–95.
[214] Hamberg M, Svensson J, Samuelsson B. Thromboxanes: a new group of biologically active compounds derived from prostaglandin endoperoxides. Proc Natl Acad Sci USA 1975;72:2994–8.
[215] Saito S, Yamasaki K, Yamada S, Matsumoto A, Akatsu T, Takahashi N, et al. A stable analogue of thromboxane $A_2$, 9,11-epithio-11,12-methanothromboxane $A_2$, stimulates bone resorption in vitro and osteoclast-like cell formation in mouse marrow culture. Bone Miner 1991;12:15–23.
[216] Shinoda J, Suzuki A, Oiso Y, Kozawa O. Thromboxane $A_2$-stimulated phospholipase D in osteoblast-like cells: possible involvement of PKC. Am J Physiol 1995;269:E524–9.
[217] Yokomizo T, Izumi T, Chang K, Takuwa Y, Shimizu T. A G-protein-coupled receptor for leukotriene $B_4$ that mediates chemotaxis. Nature 1997;387:620–4.
[218] Yokomizo T, Kato K, Terawaki K, Izumi T, Shimizu T. A second leukotriene $B_4$ receptor, BLT2. A new therapeutic target in

inflammation and immunological disorders. J Exp Med 2000;192:421–32.
[219] Yokomizo T, Izumi T, Shimizu T. Leukotriene $B_4$: metabolism and signal transduction. Arch Biochem Biophys 2001;385:231–41.
[220] Capra V, Thompson MD, Sala A, Cole DE, Folco G, Rovati GE. Cysteinyl-leukotrienes and their receptors in asthma and other inflammatory diseases: critical update and emerging trends. Med Res Rev 2007;27:469–527.
[221] Lynch KR, O'Neill GP, Liu Q, Im DS, Sawyer N, Metters KM, et al. Characterization of the human cysteinyl leukotriene CysLT1 receptor. Nature 1999;399:789–93.
[222] Heise CE, O'Dowd BF, Figueroa DJ, Sawyer N, Nguyen T, Im DS, et al. Characterization of the human cysteinyl leukotriene 2 receptor. J Biol Chem 2000;275:30531–6.
[223] Hosoi T, Koguchi Y, Sugikawa E, Chikada A, Ogawa K, Tsuda N, et al. Identification of a novel human eicosanoid receptor coupled to Gi/o. J Biol Chem 2002;277:31459–65.
[224] Gallwitz WE, Mundy GR, Lee CH, Qiao M, Roodman GD, Raftery M, et al. 5-Lipoxygenase metabolites of arachidonic acid stimulate isolated osteoclasts to resorb calcified matrices. J Biol Chem 1993;268:10087–94.
[225] Traianedes K, Dallas MR, Garrett IR, Mundy GR, Bonewald LF. 5-Lipoxygenase metabolites inhibit bone formation in vitro. Endocrinology 1998;139:3178–84.
[226] Meghji S, Sandy JR, Scutt AM, Harvey W, Harris M. Stimulation of bone resorption by lipoxygenase metabolites of arachidonic acid. Prostaglandins 1988;36:139–49.
[227] Garcia C, Boyce BF, Gilles J, Dallas M, Qiao M, Mundy GR, et al. Leukotriene $B_4$ stimulates osteoclastic bone resorption both in vitro and in vivo. J Bone Miner Res 1996;11:1619–27.
[228] Flynn MA, Qiao M, Garcia C, Dallas M, Bonewald LF. Avian osteoclast cells are stimulated to resorb calcified matrices by and possess receptors for leukotriene $B_4$. Calcif Tissue Int 1999;64:154–9.
[229] Jiang J, Lv HS, Lin JH, Jiang DF, Chen ZK. LTB4 can directly stimulate human osteoclast formation from PBMC independent of RANKL. Artif Cells Blood Substit Immobil Biotechnol 2005;33:391–403.
[230] Garcia C, Qiao M, Chen D, Kirchen M, Gallwitz W, Mundy GR, et al. Effects of synthetic peptido-leukotrienes on bone resorption in vitro. J Bone Miner Res 1996;11:521–9.
[231] Paredes Y, Massicotte F, Pelletier JP, Martel-Pelletier J, Laufer S, Lajeunesse D. Study of the role of leukotriene $B_4$ in abnormal function of human subchondral osteoarthritis osteoblasts: effects of cyclooxygenase and/or 5-lipoxygenase inhibition. Arthritis Rheum 2002;46:1804–12.
[232] Ren W, Dziak R. Effects of leukotrienes on osteoblastic cell proliferation. Calcif Tissue Int 1991;49:197–201.
[233] Klickstein LB, Shapleigh C, Goetzl EJ. Lipoxygenation of arachidonic acid as a source of polymorphonuclear leukocyte chemotactic factors in synovial fluid and tissue in rheumatoid arthritis and spondyloarthritis. J Clin Invest 1980;66:1166–70.
[234] Davidson EM, Rae SA, Smith MJ. Leukotriene $B_4$, a mediator of inflammation present in synovial fluid in rheumatoid arthritis. Ann Rheum Dis 1983;42:677–9.
[235] Ahmadzadeh N, Shingu M, Nobunaga M, Tawara T. Relationship between leukotriene $B_4$ and immunological parameters in rheumatoid synovial fluids. Inflammation 1991;15:497–503.
[236] Pelletier JP, Martel-Pelletier J, Abramson SB. Osteoarthritis, an inflammatory disease: potential implication for the selection of new therapeutic targets. Arthritis Rheum 2001;44:1237–47.
[237] Laufer S. Role of eicosanoids in structural degradation in osteoarthritis. Curr Opin Rheumatol 2003;15:623–7.
[238] Baroukh B, Saffar JS. The effect of leukotriene synthesis inhibitors on hamster periodontitis. Arch Oral Biol 1990;35(Suppl.):189S–92S.
[239] Griffiths RJ, Pettipher ER, Koch K, Farrell CA, Breslow R, Conklyn MJ, et al. Leukotriene $B_4$ plays a critical role in the progression of collagen-induced arthritis. Proc Natl Acad Sci USA 1995;92:517–21.
[240] Kuwabara K, Yasui K, Jyoyama H, Maruyama T, Fleisch JH, Hori Y. Effects of the second-generation leukotriene $B_4$ receptor antagonist, LY293111Na, on leukocyte infiltration and collagen-induced arthritis in mice. Eur J Pharmacol 2000;402:275–85.
[241] Alten R, Gromnica-Ihle E, Pohl C, Emmerich J, Steffgen J, Roscher R, et al. Inhibition of leukotriene $B_4$-induced CD11B/CD18 (Mac-1) expression by BIIL 284, a new long acting $LTB_4$ receptor antagonist, in patients with rheumatoid arthritis. Ann Rheum Dis 2004;63:170–6.
[242] Kim ND, Chou RC, Seung E, Tager AM, Luster AD. A unique requirement for the leukotriene $B_4$ receptor BLT1 for neutrophil recruitment in inflammatory arthritis. J Exp Med 2006;203:829–35.
[243] Chen M, Lam BK, Kanaoka Y, Nigrovic PA, Audoly LP, Austen KF, et al. Neutrophil-derived leukotriene $B_4$ is required for inflammatory arthritis. J Exp Med 2006;203:837–42.
[244] Shao WH, Del Prete A, Bock CB, Haribabu B. Targeted disruption of leukotriene $B_4$ receptors BLT1 and BLT2: a critical role for BLT1 in collagen-induced arthritis in mice. J Immunol 2006;176:6254–61.
[245] Marcouiller P, Pelletier JP, Guevremont M, Martel-Pelletier J, Ranger P, Laufer S, et al. Leukotriene and prostaglandin synthesis pathways in osteoarthritic synovial membranes: regulating factors for interleukin 1β synthesis. J Rheumatol 2005;32:704–12.
[246] Wittenberg RH, Willburger RE, Kleemeyer KS, Peskar BA. In vitro release of prostaglandins and leukotrienes from synovial tissue, cartilage, and bone in degenerative joint diseases. Arthritis Rheum 1993;36:1444–50.
[247] Lajeunesse D, Martel-Pelletier J, Fernandes JC, Laufer S, Pelletier JP. Treatment with licofelone prevents abnormal subchondral bone cell metabolism in experimental dog osteoarthritis. Ann Rheum Dis 2004;63:78–83.
[248] Benveniste J, Henson PM, Cochrane CG. Leukocyte-dependent histamine release from rabbit platelets. The role of IgE, basophils, and a platelet-activating factor. J Exp Med 1972;136:1356–77.
[249] Hanahan DJ. Platelet activating factor: a biologically active phosphoglyceride. Annu Rev Biochem 1986;55:483–509.
[250] Ishii S, Shimizu T. Platelet-activating factor (PAF) receptor and genetically engineered PAF receptor mutant mice. Prog Lipid Res 2000;39:41–82.
[251] Honda Z, Ishii S, Shimizu T. Platelet-activating factor receptor. J Biochem 2002;131:773–9.
[252] Honda Z, Nakamura M, Miki I, Minami M, Watanabe T, Seyama Y, et al. Cloning by functional expression of platelet-activating factor receptor from guinea-pig lung. Nature 1991;349:342–6.
[253] Ishii S, Kuwaki T, Nagase T, Maki K, Tashiro F, Sunaga S, et al. Impaired anaphylactic responses with intact sensitivity to endotoxin in mice lacking a platelet-activating factor receptor. J Exp Med 1998;187:1779–88.
[254] Ishii S, Nagase T, Shindou H, Takizawa H, Ouchi Y, Shimizu T. Platelet-activating factor receptor develops airway hyperresponsiveness independently of airway inflammation in a murine asthma model. J Immunol 2004;172:7095–102.
[255] Nagase T, Ishii S, Kume K, Uozumi N, Izumi T, Ouchi Y, et al. Platelet-activating factor mediates acid-induced lung injury in genetically engineered mice. J Clin Invest 1999;104:1071–6.
[256] Nagase T, Uozumi N, Ishii S, Kita Y, Yamamoto H, Ohga E, et al. A pivotal role of cytosolic phospholipase $A_2$ in bleomycin-induced pulmonary fibrosis. Nat Med 2002;8:480–4.
[257] Souza DG, Pinho V, Soares AC, Shimizu T, Ishii S, Teixeira MM. Role of PAF receptors during intestinal ischemia and reperfusion injury. A comparative study between PAF receptor-deficient mice and PAF receptor antagonist treatment. Br J Pharmacol 2003;139:733–40.
[258] Kihara Y, Ishii S, Kita Y, Toda A, Shimada A, Shimizu T. Dual phase regulation of experimental allergic encephalomyelitis by platelet-activating factor. J Exp Med 2005;202:853–63.
[259] Doi K, Okamoto K, Negishi K, Suzuki Y, Nakao A, Fujita T, et al. Attenuation of folic acid-induced renal inflammatory injury in

platelet-activating factor receptor-deficient mice. Am J Pathol 2006;168:1413–24.
[260] Soares AC, Pinho VS, Souza DG, Shimizu T, Ishii S, Nicoli JR, et al. Role of the platelet-activating factor (PAF) receptor during pulmonary infection with gram negative bacteria. Br J Pharmacol 2002;137:621–8.
[261] Talvani A, Santana G, Barcelos LS, Ishii S, Shimizu T, Romanha AJ, et al. Experimental *Trypanosoma cruzi* infection in platelet-activating factor receptor-deficient mice. Microbes Infect 2003;5:789–96.
[262] Rijneveld AW, Weijer S, Florquin S, Speelman P, Shimizu T, Ishii S, et al. Improved host defense against pneumococcal pneumonia in platelet-activating factor receptor-deficient mice. J Infect Dis 2004;189:711–6.
[263] Pacifici R. Estrogen, cytokines, and pathogenesis of postmenopausal osteoporosis. J Bone Miner Res 1996;11:1043–51.
[264] Kameda T, Mano H, Yuasa T, Mori Y, Miyazawa K, Shiokawa M, et al. Estrogen inhibits bone resorption by directly inducing apoptosis of the bone-resorbing osteoclasts. J Exp Med 1997;186:489–95.
[265] Cenci S, Weitzmann MN, Roggia C, Namba N, Novack D, Woodring J, et al. Estrogen deficiency induces bone loss by enhancing T-cell production of TNF-α. J Clin Invest 2000;106:1229–37.
[266] Pacifici R, Brown C, Puscheck E, Friedrich E, Slatopolsky E, Maggio D, et al. Effect of surgical menopause and estrogen replacement on cytokine release from human blood mononuclear cells. Proc Natl Acad Sci USA 1991;88:5134–8.
[267] Ammann P, Rizzoli R, Bonjour JP, Bourrin S, Meyer JM, Vassalli P, et al. Transgenic mice expressing soluble tumor necrosis factor-receptor are protected against bone loss caused by estrogen deficiency. J Clin Invest 1997;99:1699–703.
[268] Kitazawa R, Kimble RB, Vannice JL, Kung VT, Pacifici R. Interleukin-1 receptor antagonist and tumor necrosis factor binding protein decrease osteoclast formation and bone resorption in ovariectomized mice. J Clin Invest 1994;94:2397–406.
[269] Fuller K, Owens JM, Jagger CJ, Wilson A, Moss R, Chambers TJ. Macrophage colony-stimulating factor stimulates survival and chemotactic behavior in isolated osteoclasts. J Exp Med 1993;178:1733–44.
[270] Suda K, Woo JT, Takami M, Sexton PM, Nagai K. Lipopolysaccharide supports survival and fusion of preosteoclasts independent of TNF-α, IL-1, and RANKL. J Cell Physiol 2002;190:101–8.
[271] Miyazaki T, Katagiri H, Kanegae Y, Takayanagi H, Sawada Y, Yamamoto A, et al. Reciprocal role of ERK and NF-κB pathways in survival and activation of osteoclasts. J Cell Biol 2000;148:333–42.
[272] Lee SE, Chung WJ, Kwak HB, Chung CH, Kwack KB, Lee ZH, et al. Tumor necrosis factor-α supports the survival of osteoclasts through the activation of Akt and ERK. J Biol Chem 2001;276:49343–9.
[273] Wong BR, Besser D, Kim N, Arron JR, Vologodskaia M, Hanafusa H, et al. TRANCE, a TNF family member, activates Akt/PKB through a signaling complex involving TRAF6 and c-Src. Mol Cell 1999;4:1041–9.
[274] Wood DA, Hapak LK, Sims SM, Dixon SJ. Direct effects of platelet-activating factor on isolated rat osteoclasts. Rapid elevation of intracellular free calcium and transient retraction of pseudopods. J Biol Chem 1991;266:15369–76.
[275] Zheng ZG, Wood DA, Sims SM, Dixon SJ. Platelet-activating factor stimulates resorption by rabbit osteoclasts in vitro. Am J Physiol 1993;264:E74–81.
[276] Sato M, Zeng GQ, Turner CH. Biosynthetic human parathyroid hormone (1–34) effects on bone quality in aged ovariectomized rats. Endocrinology 1997;138:4330–7.
[277] Bonnick SL, Shulman L. Monitoring osteoporosis therapy: bone mineral density, bone turnover markers, or both? Am J Med 2006;119:S25–31.
[278] Kimble RB, Matayoshi AB, Vannice JL, Kung VT, Williams C, Pacifici R. Simultaneous block of interleukin-1 and tumor necrosis factor is required to completely prevent bone loss in the early postovariectomy period. Endocrinology 1995;136:3054–61.
[279] Body JJ. Calcitonin for the long-term prevention and treatment of postmenopausal osteoporosis. Bone 2002;30:75S–9S.
[280] Noguchi K, Morita I, Murota S. The detection of platelet-activating factor in inflamed human gingival tissue. Arch Oral Biol 1989;34:37–41.
[281] Pettipher ER, Higgs GA, Henderson B. PAF-acether in chronic arthritis. Agents Actions 1987;21:98–103.
[282] Palacios I, Miguelez R, Sanchez-Pernaute O, Gutierrez S, Egido J, Herrero-Beaumont G. A platelet activating factor receptor antagonist prevents the development of chronic arthritis in mice. J Rheumatol 1999;26:1080–6.
[283] Sun D, Krishnan A, Zaman K, Lawrence R, Bhattacharya A, Fernandes G. Dietary *n*−3 fatty acids decrease osteoclastogenesis and loss of bone mass in ovariectomized mice. J Bone Miner Res 2003;18:1206–16.
[284] Calder PC, Zurier RB. Polyunsaturated fatty acids and rheumatoid arthritis. Curr Opin Clin Nutr Metab Care 2001;4:115–21.
[285] Smith WL. Cyclooxygenases, peroxide tone and the allure of fish oil. Curr Opin Cell Biol 2005;17:174–82.
[286] Yamamoto S. "Enzymatic" lipid peroxidation: reactions of mammalian lipoxygenases. Free Radic Biol Med 1991;10:149–59.
[287] Serhan CN. Resolution phase of inflammation: novel endogenous anti-inflammatory and proresolving lipid mediators and pathways. Annu Rev Immunol 2007;25:101–37.
[288] Kawaguchi H, Raisz LG, Voznesensky OS, Alander CB, Hakeda Y, Pilbeam CC. Regulation of the two prostaglandin G/H synthases by parathyroid hormone, interleukin-1, cortisol, and prostaglandin $E_2$ in cultured neonatal mouse calvariae. Endocrinology 1994;135:1157–64.
[289] Chen QR, Miyaura C, Higashi S, Murakami M, Kudo I, Saito S, et al. Activation of cytosolic phospholipase $A_2$ by platelet-derived growth factor is essential for cyclooxygenase-2-dependent prostaglandin $E_2$ synthesis in mouse osteoblasts cultured with interleukin-1. J Biol Chem 1997;272:5952–8.
[290] Wadleigh DJ, Herschman HR. Transcriptional regulation of the cyclooxygenase-2 gene by diverse ligands in murine osteoblasts. Biochem Biophys Res Commun 1999;264:865–70.
[291] Koide M, Murase Y, Yamato K, Noguchi T, Okahashi N, Nishihara T. Bone morphogenetic protein-2 enhances osteoclast formation mediated by interleukin-1α through upregulation of osteoclast differentiation factor and cyclooxygenase-2. Biochem Biophys Res Commun 1999;259:97–102.

*The American Journal of Pathology, Vol. 172, No. 3, March 2008*

*DOI: 10.2353/ajpath.2008.070834*

*Cardiovascular, Pulmonary and Renal Pathology*

# Endothelial Cysteinyl Leukotriene 2 Receptor Expression Mediates Myocardial Ischemia-Reperfusion Injury

Wei Jiang,* Sean R. Hall,* Michael P.W. Moos,* Richard Yang Cao,* Satoshi Ishii,† Kofo O. Ogunyankin,‡ Luis G. Melo,*‡ and Colin D. Funk*§

*From the Departments of Physiology,* Medicine,† and Biochemistry;§ Queen's University, Kingston, Canada; and the Department of Biochemistry and Molecular Biology,‡ University of Tokyo, Tokyo, Japan*

**Cysteinyl leukotrienes (CysLTs) have been implicated as inflammatory mediators of cardiovascular disease. Three distinct CysLT receptor subtypes transduce the actions of CysLTs but the role of the endothelial CysLT$_2$ receptor (CysLT$_2$R) in cardiac function is unknown. Here, we investigated the role of CysLT$_2$R in myocardial ischemia-reperfusion (I/R) injury using transgenic (tg) mice overexpressing human CysLT$_2$R in vascular endothelium and nontransgenic (ntg) littermates. Infarction size in tg mice increased 114% compared with ntg mice 48 hours after I/R; this increase was blocked by the CysLT receptor antagonist BAY-u9773. Injection of $^{125}$I-albumin into the systemic circulation revealed significantly enhanced extravasation of the label in tg mice, indicating increased leakage of the coronary endothelium, combined with increased incidence of hemorrhage and cardiomyocyte apoptosis. Expression of proinflammatory genes such as Egr-1, VCAM-1, and ICAM was significantly increased in tg mice relative to ntg controls. Echocardiographic assessment 2 weeks after I/R revealed decreased anterior wall thickness in tg mice. Furthermore, the postreperfusion time constant $\tau$ of isovolumic relaxation was significantly increased in tg animals, indicating diastolic dysfunction. These results reveal that endothelium-targeted overexpression of CysLT$_2$R aggravates myocardial I/R injury by increasing endothelial permeability and exacerbating inflammatory gene expression, leading to accelerated left ventricular remodeling, induction of peri-infarct zone cellular apoptosis, and impaired cardiac performance.** *(Am J Pathol 2008, 172:592–602; DOI: 10.2353/ajpath.2008.070834)*

Myocardial infarction results from severe impairment of the coronary blood supply usually provoked by thrombotic or other acute alterations of coronary atherosclerotic plaque.[1] It remains the chief cause of death in North America and Europe.[2] With loss of oxygen supply, apoptosis and necrosis of cardiac myocytes in the ischemic area ensues leading to decreased cardiac performance.[1] Rapid reperfusion is essential to limit the extent of myocardial necrosis.[3] However, the consequences of reperfusion are complex and include various deleterious effects collectively referred to as ischemia-reperfusion (I/R) injury.[1] The intense inflammatory response after reperfusion plays a central role not only in promoting tissue injury, but also in repair after infarction.[4] The inflammatory process characterizing early and late reperfusion is an important aspect of the changes leading to tissue damage.[4] Increased vascular permeability and expression of adhesion molecules initiates the inflammatory reaction, and alterations of endothelial function are pivotal in the development of reperfusion damage.[4,5]

Cysteinyl leukotrienes (CysLTs), leukotriene $C_4$ ($LTC_4$), leukotriene $D_4$ ($LTD_4$), and leukotriene $E_4$ ($LTE_4$), are well established inflammatory agents that mediate bronchial and vascular smooth muscle constriction and enhance vascular permeability.[6] CysLTs are implicated in inflammatory conditions such as asthma and more recently in cardiovascular disease.[7–9] CysLTs mediate their actions via G protein-coupled receptor (GPCR) proteins, cysteinyl leukotriene 1 receptor (CysLT$_1$R), cysteinyl leukotriene 2 receptor (CysLT$_2$R), and a recently deorphanized GPCR known as

Supported by the Canadian Institutes of Health Research (grants MOP 68930 to C.D.F. and MOP 79506 to L.G.M.), the Heart and Stroke Foundation of Ontario (grant NA 5779 to L.G.M.), and the Pharmacological Society of Canada (Merck Frosst postdoctoral fellowship to S.R.H.).

This publication is dedicated to the honor of Luis G. Melo who passed away suddenly on September 26, 2007 after a brief and courageous battle with pancreatic cancer.

Accepted for publication November 20, 2007.

C.D.F. and L.G.M. hold Canada Research Chairs. C.D.F. is a career investigator of the Heart and Stroke Foundation of Ontario.

Address reprint requests to Colin D. Funk, Department of Physiology, 433 Botterell Hall, Stuart St., Queen's University, Kingston, ON K7L 3N6 Canada. E-mail: funkc@queensu.ca.

GPR17.[8,10] The $CysLT_2R$ gene is expressed in human heart and coronary vessels, also within the cardiac Purkinje system, as well as in human coronary smooth muscle cells and umbilical vein endothelial cells.[8,11–14] $CysLT_2R$ expression in mouse heart appears to be more restricted with diffuse expression within endothelial cells.[15] We generated previously transgenic (tg) mice overexpressing the human $CysLT_2R$ in vascular endothelium to characterize the role of this receptor in vascular function.[16]

The involvement of CysLTs and their receptors in inflammation and fibrosis has been confirmed in various animal and human studies.[17] Several studies reported enhanced edema and neutrophil infiltration after myocardial I/R concomitant with elevation of CysLTs.[18,19] These eicosanoids are detected as increased urinary $LTE_4$ levels in patients after admission for suspected acute myocardial infarction and unstable angina.[20] Moreover, the expression of $CysLT_1R$ and $CysLT_2R$ is increased in organs that are prone to ischemic damage and $CysLT_1R$ antagonism exerts anti-inflammatory effects on cerebral and renal I/R injury.[21–23] Few studies have investigated CysLTs and their receptors in acute myocardial infarction and specifically the role of $CysLT_2R$ in myocardial I/R injury has not been established. Here, we report that endothelium-targeted overexpression of $CysLT_2R$ aggravates myocardial I/R injury by increasing endothelial permeability and exacerbating inflammatory gene expression, leading to accelerated left ventricular (LV) remodeling and impaired cardiac performance.

## Materials and Methods

### Animals

The generation of EC-$CysLT_2R$ transgenic mice has been described previously.[16] These mice express seven copies of the human $CysLT_2R$ gene under control of the Tie2 promoter/enhancer, integrated in a gene-sparse region of chromosome 6. Hemizygous mice were continuously backcrossed with C57BL/6 mice to obtain equal numbers of transgenic and wild-type littermates. 5-Lipoxygenase-deficient ($5LO^{-/-}$) mice, developed in our laboratory previously,[24] were obtained from The Jackson Laboratory (Bar Harbor, ME). The mice were backcrossed for more than nine generations to the C57BL/6 background. The $5LO^{-/-}$ mice show absence of 5-lipoxygenase mRNA, protein, and leukotriene synthesis in inflammatory cells. $CysLT_2R$-deficient LacZ mice were generated by standard gene targeting procedures using C57BL/6 embryonic stem cells (S. Ishii, unpublished data) and embryos heterozygous for the genetic modification were transferred from Japan, revived at Queen's University, and littermates of heterozygous offspring (all on a C57BL/6 genetic background) were used in these studies.

### Mouse Model of Myocardial I/R and Drug Treatment

Mice (8 to 12 weeks) underwent coronary artery occlusion or sham surgery as previously described.[25] Briefly, mice were anesthetized with sodium pentobarbital (45 mg/kg) intraperitoneally, intubated, and ventilated with a rodent ventilator (Harvard Apparatus, St. Laurent, Canada). A midsternal thoracotomy was performed at the fourth intercostal space to expose the anterior surface of the heart. The proximal left anterior descending artery (LAD) was identified and a 6-0 silk Ethilon suture was placed around the artery and surrounding myocardium just below the atrioventricular border. Regional ischemia was induced for 30 minutes by tightening the suture against a small piece of PE-10 tubing placed on top of the LAD. Ischemia was confirmed by the discoloration of the myocardium. Sham-operated animals served as surgical controls and were subjected to the same surgical procedures as the experimental animals, with the exception that the LAD was not ligated. At the end of ischemia, the ligature was loosened and reperfusion was achieved. The lungs were reinflated and the muscle and skin layers were closed separately. The animals were weaned from the ventilator, extubated, and allowed to recover under a heat lamp before being returned to their cages. For animals receiving drug treatment, Bay-u9773 (0.25 mg/kg; Biomol Research Products, Plymouth Meeting, PA) was diluted in 1× phosphate-buffered saline (PBS) and injected intraperitoneally 4 hours before surgery, and 2, 8, and 16 hours after reperfusion. Surgical procedures and treatment regimens were approved by the University Animal Care Committee at Queen's University and adhered to the guidelines of the Canadian Council of Animal Care and the Guiding Principles in the Care and Use of Animals of the American Physiological Society.

### Morphometric Evaluation of Risk Area and Infarction Size

Forty-eight hours after reperfusion, mice were euthanized by an intraperitoneal pentobarbital overdose. The 48-hour time point was selected because it is commonly used to assess early inflammatory events (eg, leukocyte infiltration, vascular leakage). The heart was exposed and the original suture was religated. The heart was then perfused retrogradely with 100 to 200 $\mu$l of 2% Evans blue dye in PBS (pH 7.4) to delineate the nonischemic area. The heart was excised and rinsed in ice-cold PBS and the LV, including the interventricular septum, was sectioned into four or five slices of similar thickness perpendicular to the long axis of the heart. The slices were incubated in 1% 2,3,5-triphenyltetrazolium chloride (TTC; Sigma Chemicals, St. Louis, MO) at 37°C for 15 minutes to demarcate viable and necrotic tissue. The thickness of each slice was measured using calipers. The slices were photographed on both sides with a digital camera (Canon Corp., Tokyo, Japan). The infarct area (pale white), the area at risk (area excluding Evans Blue), and the total left ventricular area were traced and calculated for both sides of each slice using Image software (National Institutes of Health, Bethesda, MD). The areas for each slice were multiplied by the thickness of the slice to obtain a measure of volume. The cumulative volume for all sections for each heart was used for comparisons. The size

of LV at risk was calculated as the ratio of the LV volume excluding Evans blue dye to the total LV volume. Infarct size was calculated as the ratio of the infarct volume to the volume of the risk area as previously described.[26] Animals with infarct volume in the 35 to 70% range of total LV volume were used as inclusion criteria in the study.[27] Only one mouse was excluded based on these criteria.

### *Lactate Dehydrogenase (LDH) and Creatine Kinase (CK) Activity in Plasma*

Biochemical analysis of myocardial injury was performed in heparinized arterial blood collected at termination of the experiment. Plasma LDH and CK were measured using an automated clinical analyzer at the Kingston General Hospital using clinical grade reagents.

### *Vascular Permeability Assay in Cardiac Tissue*

Forty-eight hours after reperfusion, mice (8 to 12 weeks) were anesthetized by an intraperitoneal injection of pentobarbital (45 mg/kg). $^{125}$I-albumin ($10^6$ cpm, 1.44 mCi/mg; MP Biomedicals, Inc., Mississauga, Canada) was injected into the right external jugular vein via a PE-10 catheter. Twenty minutes after injection, the mice were euthanized, and blood was obtained as above and weighed. Exsanguination and removal of excess $^{125}$I-albumin proceeded via the right atrium. A 23-gauge needle was inserted into the apex of the left ventricle and the mouse was perfused retrogradely at 40 mmHg with 5.85 ml/100 g of 0.9% NaCl containing 100 U/ml heparin as described previously.[28] The LAD was then religated and Evans blue dye was perfused as above to delineate the risk area, which was then dissected from the remaining myocardial tissue, weighed, and placed in individual tubes. The radioactivity in the blood, nonrisk area, and risk area were counted separately using a gamma counter (Beckman Instruments, Irvine, CA). The permeability index of the different regions was calculated as the radioactivity per g of wet tissue divided by the radioactivity in 1 g of blood.[29] Sham-surgery controls were subjected to the same manipulations, with the exception that the ligature was not tied.

### *RNA Extraction and Real-Time Polymerase Chain Reaction (PCR)*

Total RNA was isolated from the risk area of the left ventricle 3 hours after reperfusion using Trizol reagent (Sigma). Total RNA was reverse-transcribed to cDNA using the Synthesis System for RT-PCR kit (Invitrogen, Carlsbad, CA) according to the manufacturer's protocol. For detection of mouse gene expression, quantitative real-time PCR was performed using a 7500 thermal cycler with TaqMan Universal PCR master mix and TaqMan gene expression assays (Egr-1, VCAM-1, and ICAM-1; Applied Biosystems, Foster City, CA) or with SYBR Green PCR master mix ($CysLT_1R$, and $CysLT_2R$) as described.[16] GAPDH was used as a control housekeeping gene. Data are calculated by the $2^{-\Delta\Delta CT}$ method and are presented as fold induction of transcripts for target genes normalized to GAPDH, with respect to the sham controls.[30]

### *Terminal Deoxynucleotidyl Transferase-Mediated dUTP Nick End-Labeling (TUNEL) Staining*

TUNEL assays were performed on LV samples with the CardioTACS *in situ* apoptosis detection kit (Trevigen, Gaithersburg, MD) as described by Takahashi and colleagues[31] with some modification. The hearts were arrested in diastole with 0.2 N KCl 48 hours after reperfusion and perfused with 3.7% neutralized formaldehyde solution. The heart was then excised, postfixed in the same fixative for another 12 hours, then cut into three sections corresponding approximately to the apex, mid-papillary, and base. The slices were embedded in paraffin, cut into 5-$\mu$m sections, and transferred to silicon-coated slides. High-power fields (12 to 20 at $\times$400 magnification) were obtained at the different levels to measure the number of TUNEL-positive cardiomyocyte nuclei in the peri-infarct border and uninfarcted remote zones, respectively. Only nuclei that were clearly located in cardiomyocytes were scored. The number of TUNEL-positive cardiomyocyte nuclei was divided by the total number of nuclei to determine the ratio of TUNEL-positive nuclei.

### *Immunohistochemical Staining*

To determine the numbers of infiltrating leukocytes, formalin-fixed, paraffin-embedded 4-$\mu$m sections were mounted on silicon-coated slides and treated with 3% $H_2O_2$ to block endogenous peroxidase. The sections were incubated for 1 hour at room temperature with rat polyclonal anti-mouse CD45 antibody (PharMingen, San Diego, CA) at a dilution of 1:50. The sections were then incubated with biotinylated rabbit IgG (Vector Laboratories, Burlingame, CA), and CD45 immunoreactivity was visualized using diaminobenzidine substrate. The number of leukocytes in the boundary area was counted in 10 random high-power fields, and the average number in each group was calculated.[32] X-gal staining to determine endogenous $CysLT_2R$ expression based on the LacZ reporter gene was performed essentially as described.[33]

### *Echocardiography*

Mice (8 to 12 weeks) underwent transthoracic echocardiography 1 day before and 2 weeks after acute I/R using a Phillips (Andover, MA) Sonos 5500 equipped with a 15-6L (15-6 MHz) intraoperative linear array transducer essentially as previously described.[34] The 2-week time point was chosen as one of the earliest time points to clearly define remodeling responses in rodents.[34] Briefly, in preparation for echocardiography, animals were lightly

anesthetized by halothane using a nose cone, shaved, and positioned on a heated pad in a recumbent position. Measurements were performed at the midpapillary level from well aligned M-mode images from the parasternal short-axis view. LVd (LV diastolic diameter), PWd (end-diastolic posterior wall thickness), and IVSd (interventricular septum thickness) were determined. The relative wall thickness for each level of the LV was calculated as (PWd + IVSd)/LVd. For each parameter, an average of five cardiac cycles was used for calculations.

### *Hemodynamic Measurements*

Two weeks after acute I/R injury, mice were anesthetized with isoflurane (2%) in medical grade oxygen. The animals were then intubated and ventilated using a pressure controlled respirator (Kent Scientific Corp., Litchfield, CN) at a tidal volume of 200 $\mu$l and a frequency of 130 strokes/minute. Body temperature was monitored with a rectal thermometer and maintained at 37°C with the aid of a heat lamp. A midsternal thoracotomy was performed as above to expose the heart. The right jugular vein was cannulated for drug administration. A 1.4F ultra-miniature Millar catheter (SPR 839; Millar Instruments, Houston, TX) was placed into the left ventricle through the apex to record LV pressure. After recording steady-state LV pressures, mice were given an intravenous administration of the synthetic catecholamine dobutamine (10 ng/g body weight) to investigate the functional integrity of adrenergic signaling in the heart. The peak hemodynamic response was recorded using a data acquisition system (PVAN, Millar Instruments). The PVAN software was used for off-line calculation of LV peak systolic pressure, LV end-diastolic pressure, LV peak-positive developed pressure ($dP/dt_{max}$), LV peak-negative developed pressure ($dP/dt_{min}$), LV pressure at peak positive developed pressure ($P@dP/dt_{max}$), heart rate, and tau ($\tau$) as described.[35] For calculation of hemodynamic parameters, a minimum of 50 consecutive cardiac cycles were used.

### *Statistical Analysis*

All data are expressed as mean ± SEM. One-way analysis of variance followed by Student-Neuman-Keuls *t*-test were used to compare differences in risk area, infarct size, myocardial enzyme activities, and endothelial permeability, as well as differences in inflammatory gene expression and cardiomyocyte apoptosis. Unpaired *t*-test was used to compare differences in neutrophil infiltration and echocardiographic and functional parameters between tg and ntg mice. Paired *t*-test was used to compare before and after I/R changes in echocardiographic parameters and LV functional responses to dobutamine in the same animals. A $P$ value $<0.05$ was considered to indicate statistical significance.

## *Results*

### *CysLT Receptor Expression in Mouse Hearts*

The expression of both native murine CysLT$_1$R and CysLT$_2$R was examined in hearts by real-time quantitative PCR as previously done in mouse ear tissue.[16] Gene expression for both CysLT receptors was low in noninfarcted ntg hearts and in infarcted hearts 3 hours after I/R injury (Figure 1). However, 48 hours after I/R injury CysLT$_1$R expression had increased 7.5-fold whereas CysLT$_2$R expression increased 3.5-fold. The human CysLT$_2$R transgene, using specific primers that can distinguish between species, could only be detected in tg mice. Using a second independent technique, we were also able to document elevation of CysLT$_2$R expression after 48 hours of I/R. Thus, using a novel mouse strain in which the *Cysltr2* gene is deleted and replaced with a LacZ reporter gene under control of the *Cysltr2* gene regulatory elements (S. Ishii et al, unpublished data) we were able to demonstrate sparse blue X-gal staining in noninfarcted ventricular tissue and 3 hours after I/R injury (Figure 1, B and C), consistent with the pattern observed previously by *in situ*

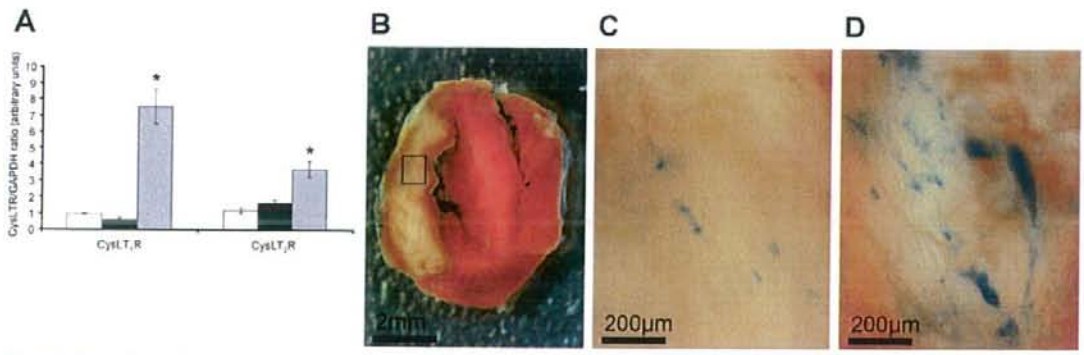


**Figure 1.** Expression of CysLT$_1$R and CysLT$_2$R in mouse hearts. **A:** Quantitative real-time PCR was used to assess gene expression for the two CysLT receptors relative to GAPDH expression in ntg mouse hearts ($n = 3$) as described in the Materials and Methods section. **Open bars**, sham-operated mice; **black bars**, hearts 3 hours after I/R; **gray bars**, hearts 48 hours after I/R. *$P < 0.05$ compared to sham-operated controls. **B:** TTC-stained heart slice from a CysLT$_2$R-deficient LacZ mouse 3 hours after I/R injury. **C:** Representative CysLT$_2$R expression in **boxed region** of the slice shown in **B** detected via the reporter gene LacZ with blue X-gal staining. **D:** CysLT$_2$R expression (via reporter LacZ/X-gal staining) in a heart slice from a CysLT$_2$R-deficient LacZ mouse having undergone 48 hours of I/R. Similar patterns of expression were observed in two additional mice at 3 and 48 hours after I/R.

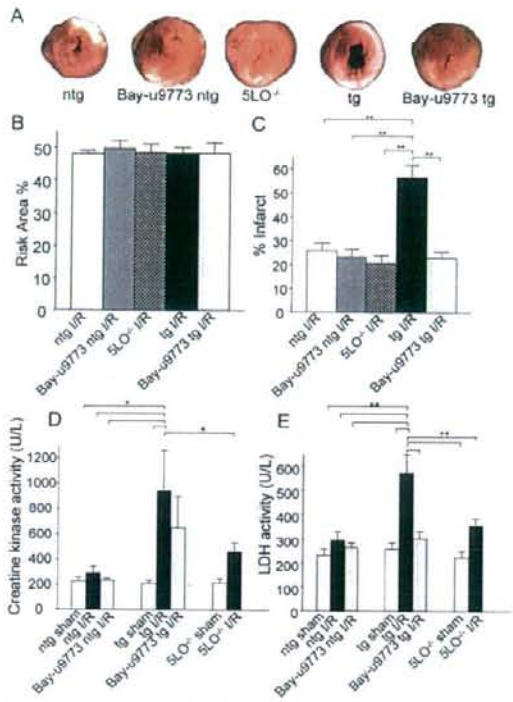


**Figure 2.** Effect of endothelial $CysLT_2R$ overexpression on LV infarct size after acute I/R injury. **A:** Representative TTC-stained ventricular sections from ntg, tg, and $5LO^{-/-}$ mice at 48 hours after I/R. Representative sections of ntg and tg mice treated with the nonselective dual $CysLT_1R/CysLT_2R$ receptor antagonist Bay-u9773 are also shown. **B:** Morphometric analysis of LV area at risk (**B**) and infarct size (**C**) in the five groups mentioned above. **D** and **E:** Serum levels of CK (**D**) and LDH (**E**) in sham and infarcted ntg, tg, and $5\text{-}LO^{-/-}$ mice at 48 hours after reperfusion. $^*P < 0.05$; $^{**}P < 0.01$; $n = 8$ for groups in **A–C**; $n = 6$ for groups in **D** and **E**.

hybridization in normal mouse heart.[15] After 48 hours of I/R injury, staining intensity increased in the infarct and peri-infarct zones (Figure 1D), which was in harmony with the PCR data.

## *Endothelial $CysLT_2R$ Overexpression Increases Myocardial Infarct Size after LAD Occlusion and Reperfusion*

The effect of endothelial overexpression of $CysLT_2R$ on myocardial I/R injury is shown in Figure 2. Gross histological analysis of TTC-stained sections 48 hours after reperfusion showed a larger necrotic area in tg animals compared to ntg littermates and 5-lipoxygenase-null $5LO^{-/-}$ mice (Figure 2A). Histomorphometric analysis revealed that infarct size in $CysLT_2R$ tg mice was increased by 114% relative to ntg mice (56 ± 15% versus 26 ± 9%, $n = 8$, $P < 0.01$) (Figure 2C), despite comparable risk area in all groups (Figure 2B). Infarct size in the $5LO^{-/-}$ null mice was comparable to ntg mice (21 ± 9% versus 26 ± 9%). Treatment of tg mice with the nonselective dual $CysLT_1R/CysLT_2R$ antagonist Bay-u9773, at a dose tested empirically to evoke $CysLT_2R$ antagonism, markedly reduced infarct size by nearly 60% (56% versus 23%, $n = 8$, $P < 0.05$) to levels comparable to ntg and $5LO^{-/-}$ mice (Figure 2, A and C). The antagonist had no additional effect on infarct size in ntg mice.

We measured serum levels of CK and LDH 48 hours after reperfusion. CK (Figure 2D) and LDH (Figure 2E) activities in infarcted ntg mice were increased by ~26% compared to the baseline levels in sham-operated controls. In contrast, CK and LDH levels were markedly elevated by 357% and 123%, respectively, in tg mice subjected to I/R compared to tg sham controls (Figure 2, D and E). Compared to ntg I/R mice, the levels of CK and LDH were elevated by ~230% and 100%, respectively, in tg mice. In concordance with the histopathological findings, treatment with Bay-u9773 reduced levels of CK and LDH after reperfusion in the tg animals (Figure 2, D and E), while having no significant effect on these markers in ntg mice. I/R increased the levels of CK and LDH in $5LO^{-/-}$ mice but this was significantly smaller than in tg mice (Figure 2, D and E).

## *Endothelial $CysLT_2R$ Overexpression Increases Permeability in the Infarcted Region of Transgenic Mouse Hearts*

Previously, we detected enhanced vascular permeability responses to leukotriene challenge and passive cutaneous anaphylaxis in mouse ear vasculature of tg mice.[16] To examine if similar vascular responses occur in the coronary endothelium after myocardial I/R, we assessed the histopathology of the infarct. In addition, we measured extravasation of $^{125}$I-BSA in the ischemic and remote areas of the left ventricle at 48 hours after reperfusion. Microscopic examination of the infarct in hematoxylin and eosin (H&E)-stained sections showed minimal accumulation of erythrocytes in the infarcted region of ntg mice (Figure 3A). In contrast, tg mice presented significant accumulation of red cells in the interstitium, resulting in hemorrhage of the infarcted area (Figure 3B). Basal coronary endothelial permeability to $^{125}$I-BSA did not differ significantly between ntg and tg mice (Figure 3C). I/R injury led to significant interstitial accumulation of $^{125}$I-BSA in both ntg and tg mice. However, the increase in coronary circulation permeability was more pronounced in tg versus ntg mice (202% versus 93%, Figure 3C). No differences in permeability were seen in the nonischemic region of the myocardium.

## *Endothelial $CysLT_2R$ Overexpression Increases $CD45^+$ Leukocyte Infiltration after I/R in Transgenic Mouse Hearts*

We used immunostaining of the pan leukocyte cell surface marker CD45 to determine whether the enhanced permeability of coronary endothelium leads to increased leukocyte infiltration of the infarcted region after I/R injury. Figure 4A shows representative cross-sections from the peri-infarct region in ntg and tg mice. The tg mice showed greater density of CD45-positive cells than ntg mice. Morphometric analysis showed

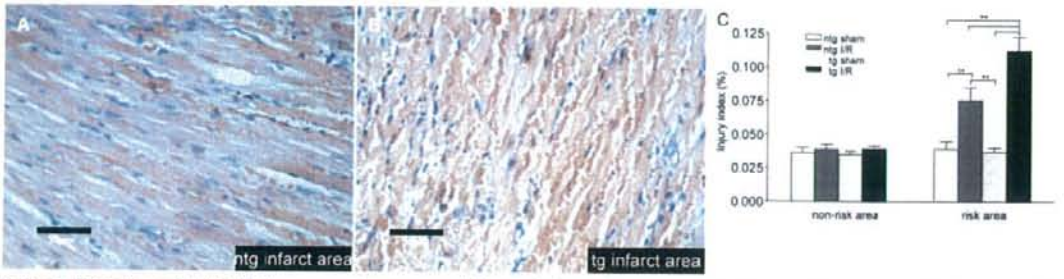


**Figure 3.** Effect of endothelial CysLT$_2$R overexpression on myocardial histopathology and coronary endothelial permeability after acute I/R injury. **A** and **B:** Microscopic appearance of infarcted left ventricle in H&E-stained paraffin sections from ntg (**A**) and tg (**B**) mice 48 hours after acute I/R injury. **C:** Permeability of coronary endothelium to $^{125}$I-BSA in the at-risk and nonrisk regions of the left ventricle of ntg and tg mice. $^{**}P < 0.01$; $n = 6$. Scale bars = 50 μm.

>100% increase in the number of infiltrating leukocytes in tg compared to ntg mice (1289 ± 113/mm$^2$ versus 528 ± 131/mm$^2$) (Figure 4).

## *Endothelial CysLT$_2$R Overexpression Increases Egr-1, ICAM, and VCAM-1 Gene Expression in Transgenic Mouse Hearts*

To examine potential molecular correlates for the I/R-induced histopathological and permeability alterations seen in tg mice, we determined myocardial mRNA expression of adhesion molecules ICAM and VCAM-1, as well as Egr-1 transcription factor (Figure 5). These genes have been implicated in the myocardial inflammatory response to I/R injury. No significant genotype-related differences were seen in basal expression of these genes. Myocardial expression of ICAM (Figure 5A), VCAM-1 (Figure 5B), and Egr-1 (Figure 5C) were increased significantly in both ntg and tg mice 3 hours after reperfusion. However, the I/R-induced increase in expression of these genes was greater in the tg mice (Figure 5).

## *Endothelial CysLT$_2$R Overexpression Increases Cardiomyocyte Apoptosis in Transgenic Mouse Hearts*

Because apoptosis plays a central role in myocardial cell loss after I/R, we determined whether endothelial overexpression of CysLT$_2$R influences the number of apoptotic nuclei in cardiomyocytes in the peri-infarct region of tg and ntg mice after I/R. We found increased apoptosis of cells with cardiomyocyte morphology in both groups at 48 hours after reperfusion (Figure 6, A and B). However, the number of apoptotic nuclei in the peri-infarct region of tg animals was significantly greater than in ntg animals (641 ± 222 TUNEL-positive myocytes/10$^4$ nuclei versus 84 ± 21/10$^4$ nuclei) (Figure 6B). At 48 hours after reperfusion, cardiomyocyte apoptosis was confined primarily to the peri-infarct region, although at earlier time points (ie, 6 to 24 hours after reperfusion), apoptosis is typically elevated in the infarct core. The number of apoptotic nuclei in the noninfarcted region was markedly lower than in the peri-infarct region and did not differ between ntg and tg mice (Figure 6B). It should be noted that apoptotic nuclei in noncardiomyocytes were observed; however, the precise cell types were not identified nor were they quantified in the present studies.

## *Endothelial CysLT$_2$R Overexpression Accelerates Left Ventricular Remodeling after I/R*

We used two-dimensional echocardiography to examine early (2 week) changes in LV wall and chamber dimensions after I/R. We chose the I/R model of myocardial infarction because it recapitulates some of the features of pathology after infarction seen in humans with reperfused MI, namely slow-developing LV remodeling that is generally complete by 3 to 6 weeks in rodents.[36,37] Repre-

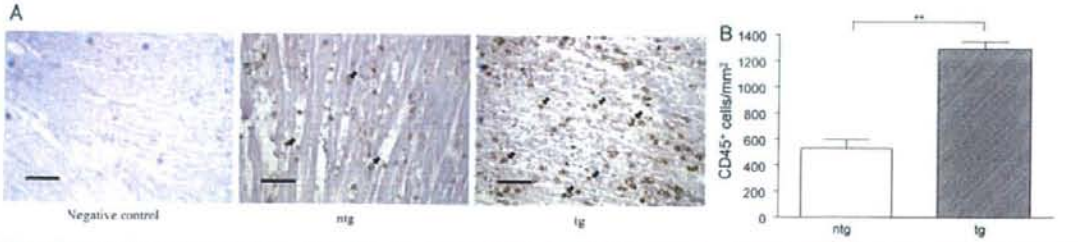


**Figure 4.** Effect of endothelial CysLT$_2$R overexpression on leukocyte infiltration after I/R. **A:** Representative photomicrographs showing immunohistochemical detection of pan-leukocyte cell surface marker CD45 in the peri-infarct region of the LV in ntg and tg mice at 48 hours after reperfusion. **Arrows** indicate CD45-positive cells. **B:** Quantitative morphometric analysis of leukocyte infiltration. $^{**}P < 0.01$; $n = 4$. Scale bars = 50 μm. Original magnifications, ×400.

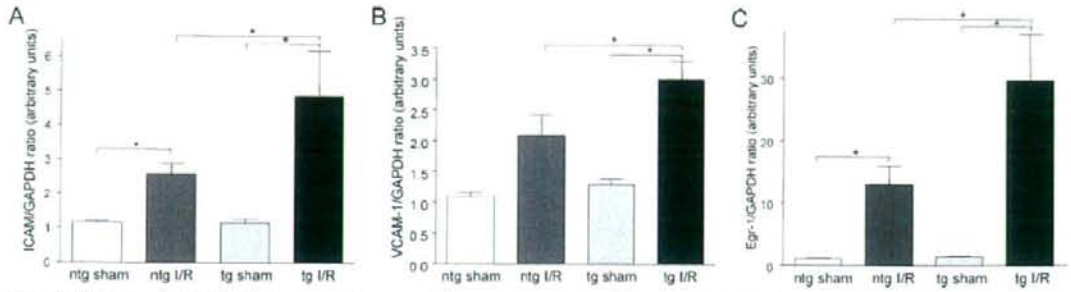


**Figure 5.** Effect of endothelial $CysLT_2R$ overexpression on proinflammatory gene expression. **A–C:** Quantitative real-time PCR evaluation of ICAM (**A**), VCAM-1 (**B**), and Egr-1 (**C**) gene expression in total RNA extracted from the ischemic area of mouse hearts at 3 hours after reperfusion. $^*P < 0.05$; $n = 3$.

sentative M-mode frames taken before and 2 weeks after acute I/R injury are shown in Figure 7, and echocardiographic data are summarized in Table 1. Pre-I/R wall and chamber dimensions did not differ significantly between ntg and tg mice, with the exception of left ventricular diastolic dimension (LVDd) that was found to be slightly increased in tg mice (Figure 7, A and C; Table 1). Two weeks after reperfusion the tg mice presented significant thinning of the anterior wall/interventricular septum, whereas the anterior wall remained relatively unchanged in ntg mice (Figure 7, B and D; Table 1). Systolic and diastolic LV chamber dimensions after infarction remained relatively unchanged from preinfarction values in ntg mice (Figure 7, C and D; Table 1). However, tg mice showed a trend toward greater LV systolic dimension after infarction than ntg mice (21% versus 12% increase with respect to preinfarction values; Figure 7, A and B, and Table 1).

### *Endothelial $CysLT_2R$ Overexpression Impairs Left Ventricular Function after I/R*

We also assessed the effect of endothelial $CysLT_2R$ overexpression on LV function using a microtip pressure catheter (Table 2). Basal LV function did not differ significantly between ntg and tg mice. Furthermore, both types of mice responded comparably to an acute bolus injection of dobutamine with increases in heart rate, LV pressures, and maximal and minimal values of the first derivative of LV pressure (Table 2). Two weeks after I/R, function remained relatively unchanged in ntg mice. In contrast, tg animals showed a trend toward decreased LV +dP/dt and LV −dP/dt and a significant increase in the time constant of isovolumic relaxation ($\tau$), indicating the presence of both systolic and diastolic dysfunction (Table 2). Interestingly, both genotypes showed refractoriness of heart rate and LV pressures to dobutamine after infarction.

## *Discussion*

The endothelium plays a pivotal role in maintaining vessel homeostasis by elaborating a variety of vasoactive, anti-inflammatory and antithrombotic factors that help maintain coronary vessel tone and protect the vessel wall against inflammatory cell and platelet adhesion.[38] Endothelial dysfunction plays a central role in the pathogenesis of myocardial I/R injury[1,5,18] and is characterized by impaired vessel relaxation, and enhanced expression of

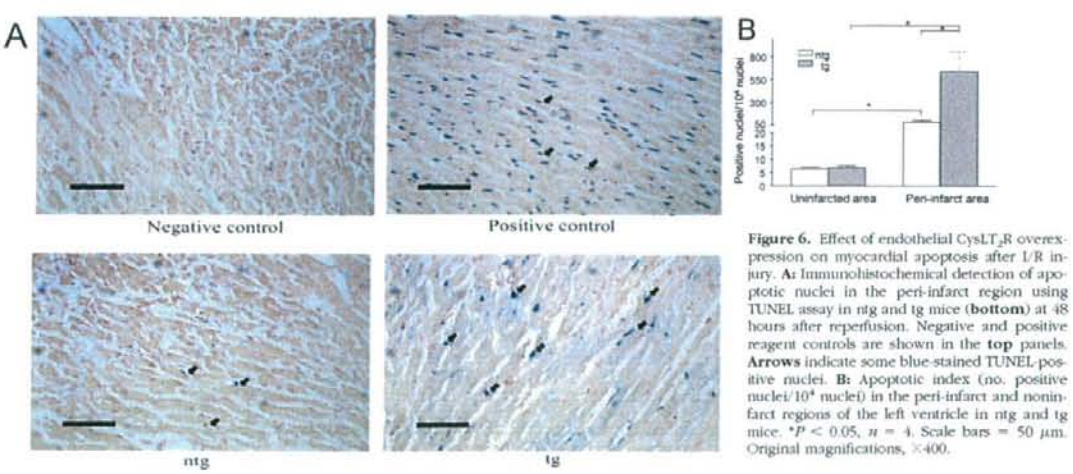


**Figure 6.** Effect of endothelial $CysLT_2R$ overexpression on myocardial apoptosis after I/R injury. **A:** Immunohistochemical detection of apoptotic nuclei in the peri-infarct region using TUNEL assay in ntg and tg mice (**bottom**) at 48 hours after reperfusion. Negative and positive reagent controls are shown in the **top** panels. **Arrows** indicate some blue-stained TUNEL-positive nuclei. **B:** Apoptotic index (no. positive nuclei/$10^4$ nuclei) in the peri-infarct and noninfarct regions of the left ventricle in ntg and tg mice. $^*P < 0.05$, $n = 4$. Scale bars = 50 μm. Original magnifications, ×400.

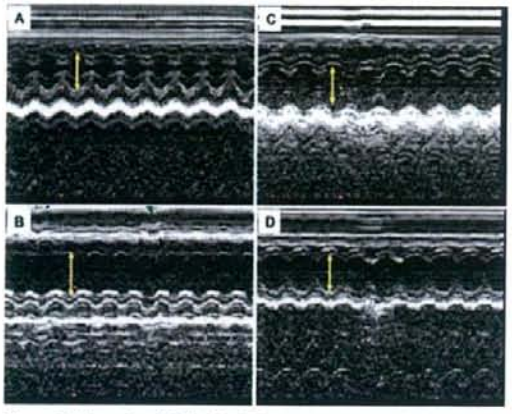


**Figure 7.** Effect of endothelial CysLT$_2$R overexpression on left ventricular wall and chamber dimensions. **A–D:** Representative M-mode frames from the mid-papillary region of tg (**A**, **B**) and ntg (**C**, **D**) before (**A**, **C**) and 2 weeks after (**B**, **D**) acute I/R injury. **Arrow** indicates width of the LV chamber.

inflammatory and adhesion molecules, leading to increased vascular permeability, inflammatory cell infiltration, and platelet adhesion and thrombus formation.[5] CysLTs are major inflammatory mediators and activation of endothelial CysLT$_2$R markedly increases vascular permeability in transgenic mice.[16] We now report that myocardial injury in response to acute I/R is exacerbated in endothelium-targeted CysLT$_2$R transgenic mice, in association with increased coronary vascular permeability, inflammatory cell infiltration, and heightened myocyte loss through apoptosis.

CysLT synthesis increases in humans[20] with myocardial infarction. Furthermore, pretreatment with leukotriene biosynthesis inhibitors, AA-861 or Bay X1005, reduces neutrophil influx and infarct size after I/R injury in rats[39] and rabbits,[40] respectively, and intravenous infusion of a CysLT receptor antagonist LY-171883 at reperfusion decreases infarct size and improves LV functional recovery after myocardial infarction in cats.[41] In addition, recent linkage analysis studies revealed increased risk of stroke and myocardial infarction in some ethnic groups harboring a distinct haplotype in the *ALOX5AP* gene encoding 5-lipoxygenase-activating protein.[42] Thus, it is plausible in the current study that CysLTs released from resident and/or circulating inflammatory cells or synthesized by transcellular pathways between interacting neutrophils and endothelial cells[40,43] may activate CysLT$_2$Rs in vascular endothelium to promote endothelial leakage and subsequent myocardial damage. CysLTs influence the adhesion of neutrophils to endothelium by up-regulating adhesion molecules[44,45] and may also act as chemotactic factors in recruitment of leukocytes to the infarcted myocardium. There is compelling evidence that activation of CysLT$_2$R in cultured human endothelial cells leads to activation of a distinct set of immediate-early gene signatures[46] including the transcription factor Egr-1 and a variety of signaling and adhesion molecules that have been shown to participate in ischemic stress and reperfusion injury in mice.[47] In agreement with these findings, the expression of Egr-1, as well as ICAM and VCAM-1 genes, were elevated in the present study after activation of the human transgene in vascular endothelium, suggesting that they may contribute to the enhanced endothelial permeability and neutrophil infiltration in the infarcted myocardium of tg mice.

To examine the relative impact of transgenic endothelial overexpression of CysLT$_2$ receptor vis-à-vis native CysLT$_2$ expression after I/R, a number of tests were performed including analysis of the expression level of CysLT$_1$ and CysLT$_2$ receptors before and after injury (Figure 1), as well as comparative analysis of treatment with the dual CysLT$_1$/CysLT$_2$ receptor antagonist Bay-u9773, combined with infarction analysis of 5LO/leukotriene-deficient mice (Figure 2). Real-time PCR analysis indicated low levels of native murine CysLT$_1$ and CysLT$_2$ receptors in sham-operated mouse hearts and early after I/R (3 hours) with significantly higher levels of both receptors 48 hours after I/R. We speculate that the increased CysLT$_1$R levels at 48 hours of I/R are attributable to infiltrating mononuclear leukocytes, a predominant cell type at this time point[32] and cells known to express this receptor subtype.[48] Based on the blue X-gal/LacZ staining in heart tissue as a surrogate for CysLT$_2$R expression, enhanced expression of this receptor subtype after 48 hours of I/R in the infarct and peri-infarct zones was observed (Figure 1). Although the specific cell types expressing the induced receptor were not positively identified, several cell types including vascular smooth muscle[12] and endothelial cells,[15] Purkinje conducting cells,[11]

**Table 1.** Two-Dimensional Echocardiographic Analysis of Left Ventricular Wall and Chamber Dimension before and 2 Weeks after Acute Myocardial I/R in CysLT$_2$R Transgenic and Nontransgenic Mice

| | Pre-ischemia/reperfusion | | Post-ischemia/reperfusion | | % change from pre I/R | |
|---|---|---|---|---|---|---|
| | ntg | tg | ntg | tg | ntg | tg |
| LVDd (mm) | 0.350 ± 0.010 | 0.389 ± 0.0120* | 0.378 ± 0.0087 | 0.424 ± 0.0300 | 8.6 ± 4.4 | 8.8 ± 6.5 |
| LVDs (mm) | 0.200 ± 0.0090 | 0.229 ± 0.0173 | 0.220 ± 0.0185 | 0.27 ± 0.0342 | 11.5 ± 10.2 | 20.9 ± 15.9 |
| IVSd (mm) | 0.0751 ± 0.0030 | 0.0707 ± 0.0022 | 0.0727 ± 0.0025 | 0.0712 ± 0.0008 | −2.6 ± 4.0 | 1.3 ± 3.8 |
| IVSs (mm) | 0.127 ± 0.0047 | 0.125 ± 0.0083 | 0.118 ± 0.0085 | 0.103 ± 0.0067† | −6.1 ± 8.8 | −16.9 ± 4.3 |
| PWd (mm) | 0.0719 ± 0.0017 | 0.0763 ± 0.0044 | 0.0811 ± 0.0045 | 0.0867 ± 0.0041 | 13.9 ± 8.4 | 16.7 ± 11.2 |
| PWs (mm) | 0.124 ± 0.0052 | 0.125 ± 0.0044 | 0.143 ± 0.0148 | 0.148 ± 0.0060† | 15.9 ± 11.4 | 19.6 ± 7.6 |
| HR (bpm) | 472 ± 17 | 479 ± 30 | 476 ± 21 | 481 ± 40 | 1.2 ± 4.9 | 0.30 ± 4.6 |

LVDd, left ventricular chamber diameter at diastole; LVDs, left ventricular chamber diameter at systole; IVSd, interventricular septum thickness at diastole; IVSs, interventricular septum thickness at systole; PWd, posterior wall thickness at diastole; PWs, posterior wall thickness at systole; HR, heart rate. *$P < 0.05$, tg versus ntg by unpaired *t*-test; †$P < 0.05$, pre-I/R versus post-I/R by paired *t*-test.

**Table 2.** Left Ventricular Function in Control $CysLT_2R$-Transgenic and Nontransgenic Mice and 2 Weeks after Acute Myocardial I/R Injury

| | ntg | | | | tg | | | |
|---|---|---|---|---|---|---|---|---|
| | Control ($n$ = 6) | | I/R ($n$ = 5) | | Control ($n$ = 5) | | I/R ($n$ = 5) | |
| | Before DB | After DB | Before DB | After DB | Before DB | After DB | Before DB | After DB |
| Heart rate, beats/minute | 633 ± 14 | 709 ± 17* | 616 ± 26 | 664 ± 44 | 575 ± 13‡ | 642 ± 11*‡ | 519 ± 32‡ | 522 ± 39*‡ |
| LV function | | | | | | | | |
| LV peak pressure, mmHg | 71 ± 2 | 138 ± 13* | 69 ± 4 | 72 ± 3 | 74 ± 4 | 130 ± 14* | 70 ± 4 | 83 ± 8 |
| LVESP, mmHg | 70 ± 2 | 138 ± 13* | 68 ± 4 | 71 ± 3 | 72 ± 4 | 130 ± 14* | 70 ± 4* | 83 ± 8† |
| LVEDP, mmHg | 3 ± 0 | 5 ± 1 | 3 ± 0.3 | 4 ± 0.4 | 5 ± 1 | 7 ± 1* | 4 ± 0.6 | 4 ± 0.2 |
| LV +dP/dt, mmHg/second | 5636 ± 320 | 16,046 ± 1281* | 6409 ± 425 | 9952 ± 1557*† | 6571 ± 604 | 13,921 ± 1867* | 4896 ± 569 | 7412 ± 1728† |
| LV −dP/dt, mm Hg/second | −6058 ± 423 | −10,377 ± 648* | −6624 ± 489 | −6454 ± 397† | −6267 ± 621 | −9144 ± 680* | −4865 ± 662 | −5370 ± 735† |
| $\tau$, ms | 6.37 ± 0.44 | 5.10 ± 0.19* | 5.91 ± 0.33 | 4.94 ± 0.17* | 5.76 ± 0.22 | 5.77 ± 0.20‡ | 7.91 ± 0.82† | 7.17 ± 0.77‡ |

DB, dobutamine; LV, left ventricle; LVESP, left ventricular end-systolic pressure; LVEDP, left ventricular end-diastolic pressure; LV +dP/dt, maximal value of the first derivative of LV pressure; LV −dP/dt, minimal value of the first derivative of LV pressure; $\tau$, time constant for isovolumic relaxation.
*$P < 0.05$ after DB versus before DB; †$P < 0.05$, control versus I/R; ‡$P < 0.05$ tg versus ntg.

mesenchymal stem cells, and perhaps some leukocytes are possible candidates.

Bay-u9773 is a nonspecific antagonist of $CysLT_1R$ and $CysLT_2R$, rendering it difficult to determine the precise contributions of each receptor subtype to ischemic injury. This is further complicated by the recent discovery of a third CysLT receptor subtype termed GPR17, that can bind $CysLT_1R$ antagonists and was found to participate in focal rat brain ischemic injury.[10] Therefore, depending on the organ and tissue-specific vascular beds, various CysLT receptor subtypes might contribute to inflammatory vascular permeability changes in ischemic injury. In our studies, absence of leukotriene ligand to $CysLT_2R$, as represented in 5LO-deficient mice, and in preliminary studies with the recently acquired $CysLT_2R$-deficient LacZ mice ($n$ = 3, data not shown), lack of ligand/receptor did not significantly influence myocardial injury compared to ntg mice. These data are consistent with those in a recent study showing that I/R injury did not differentially affect infarct size in 5LO-deficient mice compared to wild-type controls[49] but apparently not in agreement with the studies mentioned above with leukotriene biosynthesis inhibitors.[39,40] Moreover, the finding that Bay-u9773 did not reduce infarct size below baseline levels in ntg mice suggests that endogenous $CysLT_2R$ does not play a significant role in I/R injury in contrast to the transgenic overexpression of the receptor. However, the observation that I/R induces murine $CysLT_2R$ in our study at 48 hours, along with a recent report examining $CysLT_2R$ expression in human brain tissue finding increased expression in microvascular endothelium after traumatic injury,[50] warrants further study to examine the pathophysiological sequelae of induction of $CysLT_2R$.

The mechanism by which endothelial $CysLT_2R$ overexpression leads to increased myocyte apoptosis is not known. To our knowledge no direct role of $CysLT_2R$ in cardiomyocyte apoptosis has been established. The cascade of events leading to myocyte apoptosis during I/R involves the activation of both the intrinsic mitochondrial proapoptotic pathway as well as the extrinsic pathway mediated by cytokine activation of death receptors.[51] Myocytes are particularly prone to apoptosis during reperfusion,[52] where up to 30% in the risk area may undergo apoptosis in the first few hours after reperfusion. The events of reperfusion that lead to cardiomyocyte apoptosis have not been fully elucidated. However, reactive oxygen species and cytokines produced by infiltrating inflammatory cells appear to play a central role in activating apoptotic pathways in myocytes.[52,53] For example, genetic mouse models harboring deletions of tumor necrosis factor-$\alpha$ and CD18 genes show reduced infarct size in response to I/R in association with decreased neutrophil infiltration, whereas null mice for the anti-oxidant gene heme oxygenase-1 have increased infarct size and reduced LV recovery in parallel with a decrease in antioxidant load.[52] In the current study, the enhanced influx of $CD45^+$ leukocytes, presumably mostly neutrophils, after reperfusion in $CysLT_2R$ tg mice could potentially contribute to the enhanced myocyte apoptosis seen in these animals by a similar mechanism; however, additional mechanisms may also be at play. Regardless of mechanism, the increased apoptosis in tg mice would predictably lead to greater long-term loss of myocardial contractile mass, resulting in LV chamber remodeling and impairment of contractile function. Indeed, in the current study, $CysLT_2R$ mice show accelerated LV remodeling, highlighted by decreased anterior wall thickness and increased LV systolic dimensions 2 weeks after reperfusion. Typically, LV remodeling in mice with reperfused myocardium is slow and often absent,[37]

unless a significant amount of the LV (>40% of the area at risk) is infarcted. Our results indicate that tg CysLT$_2$R mice had significantly larger infarcts than the ntg counterparts. We presume that the heightened apoptosis is, at least partially, responsible for the larger infarct sizes and subsequent LV remodeling in these mice.

As expected, LV remodeling in tg mice was accompanied by impaired LV function after reperfusion. We believe that this is directly attributable to the greater myocyte loss in tg mice, because basal LV function and responsiveness to $\beta$-adrenergic stimulation did not differ significantly between the two groups of animals. In contrast, ntg mice were able to preserve LV function after reperfusion because of the significantly smaller infarcts and absence of negative remodeling. Interestingly, both genotypes showed marked refractoriness to dobutamine after reperfusion. The mechanism underlying this lack of response appears to be unrelated to CysLT$_2$R overexpression, because it is also present in ntg controls. $\beta$-Adrenergic receptor desensitization usually occurs after myocardial infarction as the sympathetic nervous system attempts to maintain hemodynamic homeostasis. However, desensitization usually occurs throughout a longer time course than in the current studies, and is unlikely to be the explanation for the postreperfusion refractoriness to dobutamine.

In summary, the results of the current study indicate that endothelial-targeted overexpression of CysLT$_2$R exacerbates myocardial injury after ischemia reperfusion in association with increased inflammatory cell infiltration and cardiomyocyte apoptosis. Inhibition of endothelial CysLT$_2$R activity should be explored further as a potential strategy for myocardial protection.

## *Acknowledgments*

We thank Karoline Machado and the staff at the Queen's University Transgenic Animal Facility for performing the embryo transfer procedures to obtain CysLT$_2$R-deficient LacZ mice. Yiqun Hui is kindly acknowledged for supplying the CysLT$_2$R transgenic mice.

## *References*

1. Buja LM: Myocardial ischemia and reperfusion injury. Cardiovasc Pathol 2005, 14:170–175
2. Moens AL, Claeys MJ, Timmermans JP, Vrints CJ: Myocardial ischemia/reperfusion-injury, a clinical view on a complex pathophysiological process. Int J Cardiol 2005, 100:179–190
3. Park JL, Lucchesi BR: Mechanisms of myocardial reperfusion injury. Ann Thorac Surg 1999, 68:1905–1912
4. Di Napoli P, Taccardi AA, De Caterina R, Barsotti A: Pathophysiology of ischemia-reperfusion injury: experimental data. Ital Heart J 2002, 3(Suppl 4):24S–28S
5. Lefer AM, Tsao PS, Lefer DJ, Ma XL: Role of endothelial dysfunction in the pathogenesis of reperfusion injury after myocardial ischemia. FASEB J 1991, 5:2029–2034
6. Funk CD: Prostaglandins and leukotrienes: advances in eicosanoid biology. Science 2001, 294:1871–1875
7. Funk CD: Leukotriene modifiers as potential therapeutics for cardiovascular disease. Nat Rev Drug Disc 2005, 4:664–672
8. Hui Y, Funk CD: Cysteinyl leukotriene receptors. Biochem Pharmacol 2002, 64:1549–1557
9. Folco G, Rossoni G, Buccellati C, Berti F, Maclouf J, Sala A: Leukotrienes in cardiovascular diseases. Am J Respir Crit Care Med 2000, 161:S112–S116
10. Ciana P, Fumagalli M, Trincavelli ML, Verderio C, Rosa P, Lecca D, Ferrario S, Parravicini C, Capra V, Gelosa P, Guerrini U, Belcredito S, Cimino M, Sironi L, Tremoli E, Rovati GE, Martini C, Abbracchio MP: The orphan receptor GPR17 identified as a new dual uracil nucleotides/cysteinyl-leukotrienes receptor. EMBO J 2006, 25:4615–4627
11. Heise CE, O'Dowd BF, Figueroa DJ, Sawyer N, Nguyen T, Im DS, Stocco R, Bellefeuille JN, Abramovitz M, Cheng R, Williams DL Jr, Zeng Z, Liu Q, Ma L, Clements MK, Coulombe N, Liu Y, Austin CP, George SR, O'Neill GP, Metters KM, Lynch KR, Evans JF: Characterization of the human cysteinyl leukotriene 2 receptor. J Biol Chem 2000, 275:30531–30536
12. Takasaki J, Kamohara M, Matsumoto M, Saito T, Sugimoto T, Ohishi T, Ishii H, Ota T, Nishikawa T, Kawai Y, Masuho Y, Isogai T, Suzuki Y, Sugano S, Furuichi K: The molecular characterization and tissue distribution of the human cysteinyl leukotriene CysLT(2) receptor. Biochem Biophys Res Commun 2000, 274:316–322
13. Lötzer K, Spanbroek R, Hildner M, Urbach A, Heller R, Bretschneider E, Galczenski H, Evans JF, Habenicht AJ: Differential leukotriene receptor expression and calcium responses in endothelial cells and macrophages indicate 5-lipoxygenase-dependent circuits of inflammation and atherogenesis. Arterioscler Thromb Vasc Biol 2003, 23:e32–e36
14. Kamohara M, Takasaki J, Matsumoto M, Matsumoto SI, Saito T, Soga T, Matsushime H, Furuichi K: Functional characterization of cysteinyl leukotriene CysLT(2) receptor on human coronary artery smooth muscle cells. Biochem Biophys Res Commun 2001, 287:1088–1092
15. Hui Y, Yang G, Galczenski H, Figueroa DJ, Austin CP, Copeland NG, Gilbert DJ, Jenkins NA, Funk CD: The murine cysteinyl leukotriene 2 (CysLT2) receptor, cDNA and genomic cloning, alternative splicing, and in vitro characterization. J Biol Chem 2001, 276:47489–47495
16. Hui Y, Cheng Y, Smalera I, Jian W, Goldhahn L, Fitzgerald GA, Funk CD: Directed vascular expression of human cysteinyl leukotriene 2 receptor modulates endothelial permeability and systemic blood pressure. Circulation 2004, 110:3360–3366
17. Kanaoka Y, Boyce JA: Cysteinyl leukotrienes and their receptors: cellular distribution and function in immune and inflammatory responses. J Immunol 2004, 173:1503–1510
18. Frangogiannis NG, Smith CW, Entman ML: The inflammatory response in myocardial infarction. Cardiovasc Res 2002, 53:31–47
19. Barst S, Mullane K: The release of a leukotriene D4-like substance following myocardial infarction in rabbits. Eur J Pharmacol 1985, 114:383–387
20. Carry M, Korley V, Willerson JT, Weigelt L, Ford-Hutchinson AW, Tagari P: Increased urinary leukotriene excretion in patients with cardiac ischemia. In vivo evidence for 5-lipoxygenase activation. Circulation 1992, 85:230–236
21. Yu GL, Wei EQ, Zhang SH, Xu HM, Chu LS, Zhang WP, Zhang Q, Chen Z, Mei RH, Zhao MH: Montelukast, a cysteinyl leukotriene receptor-1 antagonist, dose- and time-dependently protects against focal cerebral ischemia in mice. Pharmacology 2005, 73:31–40
22. Fang SH, Zhou Y, Chu LS, Zhang WP, Wang ML, Yu GL, Peng F, Wei EQ: Spatio-temporal expression of cysteinyl leukotriene receptor-2 mRNA in rat brain after focal cerebral ischemia. Neurosci Lett 2007, 412:78–83
23. Sener G, Sehirli O, Velioglu-Oguncc A, Cetinel S, Gedik N, Caner M, Sakarcan A, Yegen BC: Montelukast protects against renal ischemia/reperfusion injury in rats. Pharmacol Res 2006, 54:65–71
24. Chen XS, Sheller JR, Johnson EN, Funk CD: Role of leukotrienes revealed by targeted disruption of the 5-lipoxygenase gene. Nature 1994, 372:179–182
25. Tarnavski O, McMullen JR, Schinke M, Nie Q, Kong S, Izumo S: Mouse cardiac surgery: comprehensive techniques for the generation of mouse models of human diseases and their application for genomic studies. Physiol Genom 2004, 16:349–360
26. Liu X, Wei J, Peng DH, Layne MD, Yet SF: Absence of heme oxygenase-1 exacerbates myocardial ischemia/reperfusion injury in diabetic mice. Diabetes 2005, 54:778–784
27. Petzelbauer P, Zacharowski PA, Miyazaki Y, Friedl P, Wickenhauser G, Castellino FJ, Groger M, Wolff K, Zacharowski K: The fibrin-derived peptide Bbeta15-42 protects the myocardium against ischemia-reperfusion injury. Nat Med 2005, 11:298–304
28. Schumacher J, Binkowski K, Dendorfer A, Klotz KF: Organ-specific

extravasation of albumin-bound Evans blue during nonresuscitated hemorrhagic shock in rats. Shock 2003, 20:565–568
29. Younger JG, Sasaki N, Delgado J, Ko AC, Nghiem TX, Waite MD, Till GO, Ward PA: Systemic and lung physiological changes in rats after intravascular activation of complement. J Appl Physiol 2001, 90:2289–2295
30. Harja E, Bucciarelli LG, Lu Y, Stern DM, Zou YS, Schmidt AM, Yan SF: Early growth response-1 promotes atherogenesis: mice deficient in early growth response-1 and apolipoprotein E display decreased atherosclerosis and vascular inflammation. Circ Res 2004, 94:333–339
31. Takahashi T, Tang T, Lai NC, Roth DM, Rebolledo B, Saito M, Lew WY, Clopton P, Hammond HK: Increased cardiac adenylyl cyclase expression is associated with increased survival after myocardial infarction. Circulation 2006, 114:388–396
32. Dewald O, Ren G, Duerr GD, Zoerlein M, Klemm C, Gersch C, Tincey S, Michael LH, Entman ML, Frangogiannis NG: Of mice and dogs: species-specific differences in the inflammatory response following myocardial infarction. Am J Pathol 2004, 164:665–677
33. Okada Y, Scott G, Ray MK, Mishina Y, Zhang Y: Histone demethylase JHDM2A is critical for Tnp1 and Prm1 transcription and spermatogenesis. Nature 2007, 450:119–123
34. Liu X, Simpson JA, Brunt KR, Ward CA, Hall SR, Kinobe RT, Barrette V, Tse MY, Pang SC, Pachori AS, Dzau VJ, Ogunyankin K, Melo LG: Pre-emptive heme oxygenase-1 gene delivery reveals reduced mortality and preservation of left ventricular function one year after acute myocardial infarction. Am J Physiol 2007, 293:H48–H59
35. Hall SR, Wang L, Milne B, Hong M: Left ventricular dysfunction after acute intracranial hypertension is associated with increased hydroxyl free radical production, cardiac ryanodine hyperphosphorylation, and troponin I degradation. J Heart Lung Transplant 2005, 24:1639–1649
36. Anversa P, Beghi C, Kikkawa Y, Olivetti G: Myocardial infarction in rats. Infarct size, myocyte hypertrophy and capillary growth. Circ Res 1986, 58:26–37
37. De Celle T, Cleutjens JP, Balnkesteijn WM, Debets JJ, Smits JF, Janssen BJ: Long-term structural and functional consequences of cardiac ischemia-reperfusion injury in vivo in mice. Exp Physiol 2004, 89:605–615
38. Rubanyi GM: The role of endothelium in cardiovascular homeostasis and disease. J Cardiovasc Pharmacol 1993, 22:S1–S4
39. Sasaki K, Ueno A, Kswamura M, Katori M, Shigehiro S, Kikawada R: Reduction of myocardial infarct size in rats by selective 5-lipooxygenase inhibitor (AA-861). Adv Prostglandin Thromboxane Leukot Res 1987, 17A:381–383
40. Rossoni G, Sala A, Berti F, Testa T, Buccellati C, Molta C, Muller-Peddinghaus R, Maclouf J, Folco GC: Myocardial protection by the leukotriene synthesis inhibitor BAY X1005: importance of transcellular biosynthesis of cysteinyl-leukotrienes. J Pharmacol Exp Ther 1996, 276:335–341
41. Hock CE, Beck LD, Papa LA: Peptide leukotriene antagonism in myocardial ischemia and reperfusion. Cardiovasc Res 1992, 26:1206–1211
42. Helgadottir A, Manolescu A, Thorleifsson G, Gretarsdottir S, Jonsdottir H, Thorsteinsdottir U, Samani NJ, Gudmundsson G, Grant SF, Thorgeirsson G, Sveinbjornsdottir S, Valdimarsson EM, Matthiasson SE, Johannsson H, Gudmundsdottir O, Gurney ME, Sainz J, Thorhallsdottir M, Andresdottir M, Frigge ML, Topol EJ, Kong A, Gudnason V, Hakonarson H, Gulcher JR, Stefansson K: The gene encoding 5-lipoxygenase activating protein confers risk of myocardial infarction and stroke. Nat Genet 2004, 36:233–239
43. Sala A, Folco G: Neutrophils, endothelial cells, and cysteinyl leukotrienes: a new approach to neutrophil-dependent inflammation? Biochem Biophys Res Commun 2001, 283:1003–1006
44. Pedersen KE, Bochner BS, Undem BJ: Cysteinyl leukotrienes induce P-selectin expression in human endothelial cells via a non-CysLT1 receptor-mediated mechanism. J Pharmacol Exp Ther 1997, 281:655–662
45. Di Gennaro A, Carnini C, Buccellati C, Ballerio R, Zarini S, Fumagalli F, Viappiani S, Librizzi L, Hernandez A, Murphy RC, Constantin G, De Curtis M, Folco G, Sala A: Cysteinyl-leukotrienes receptor activation in brain inflammatory reactions and cerebral edema formation: a role for transcellular biosynthesis of cysteinyl-leukotrienes. FASEB J 2004, 18:842–844
46. Uzonyi B, Lotzer K, Jahn S, Kramer C, Hildner M, Bretschneider E, Radke D, Beer M, Vollandt R, Evans JF, Funk CD, Habenicht AJ: Cysteinyl leukotriene 2 receptor and protease-activated receptor 1 activate strongly correlated early genes in human endothelial cells. Proc Natl Acad Sci USA 2006, 103:6326–6331
47. Yan SF, Fujita T, Lu J, Okada K, Shan Zou Y, Mackman N, Pinsky DJ, Stern DM: Egr-1, a master switch coordinating upregulation of divergent gene families underlying ischemic stress. (Erratum in: Nat Med 2001, 7:509). Nat Med 2000, 6:1355–1361
48. Figueroa DJ, Breyer RM, Defoe SK, Kargman S, Daugherty BL, Waldburger K, Liu Q, Clements M, Zeng Z, O'Neill GP, Jones TR, Lynch KR, Austin CP, Evans JF: Expression of the cysteinyl leukotriene 1 receptor in normal human lung and peripheral blood leukocytes. Am J Respir Crit Care Med 2001, 163:226–233
49. Adamek A, Jung S, Dienesch C, Laser M, Ertl G, Bauersachs J, Frantz S: Role of 5-lipoxygenase in myocardial ischemia-reperfusion injury in mice. Eur J Pharmacol 2007, 57:51–54
50. Hu H, Chen G, Zhang JM, Zhang WP, Zhang L, Ge QF, Yao HT, Ding W, Chen Z, Wei EQ: Distribution of cysteinyl leukotriene receptor 2 in human traumatic brain injury and brain tumors. Acta Pharmacol Sin 2005, 26:685–690
51. Crow MT, Mani K, Nam Y-J, Kitsis RN: The mitochondrial death pathway and cardiac myocyte apoptosis. Circ Res 2004, 95:957–970
52. Eefting F, Rensing B, Wigman J, Pannekoek WJ, Liu WM, Cramer MJ, Lips DJ, Doevendans PA: Role of apoptosis in reperfusion injury. Cardiovasc Res 2004, 61:414–426
53. Duilio C, Ambrosio G, Kuppusamy P, DiPaula A, Becker LC, Zweier JL: Neutrophils are primary source of O2 radicals during reperfusion after prolonged myocardial ischemia. Am J Physiol 2001, 280:H2649–H2657

# Platelet-Activating Factor Production in the Spinal Cord of Experimental Allergic Encephalomyelitis Mice via the Group IVA Cytosolic Phospholipase $A_2$-Lyso-PAFAT Axis[1]

**Yasuyuki Kihara,* Keisuke Yanagida,* Kayo Masago,* Yoshihiro Kita,* Daisuke Hishikawa,* Hideo Shindou,* Satoshi Ishii,*† and Takao Shimizu[2]***

**Platelet-activating factor (PAF; 1-*O*-alkyl-2-acetyl-*sn*-glycero-3-phosphocholine) plays a critical role in inflammatory disorders including experimental allergic encephalomyelitis (EAE), an animal model for multiple sclerosis (MS). Although PAF accumulation in the spinal cord (SC) of EAE mice and cerebrospinal fluid of MS patients has been reported, little is known about the metabolic processing of PAF in these diseases. In this study, we demonstrate that the activities of phospholipase $A_2$ ($PLA_2$) and acetyl-CoA:lyso-PAF acetyltransferase (LysoPAFAT) are elevated in the SC of EAE mice on a C57BL/6 genetic background compared with those of naive mice and correlate with disease severity. Correspondingly, levels of groups IVA, IVB, and IVF cytosolic $PLA_2$s, group V secretory $PLA_2$, and LysoPAFAT transcripts are up-regulated in the SC of EAE mice. PAF acetylhydrolase activity is unchanged during the disease course. In addition, we show that LysoPAFAT mRNA and protein are predominantly expressed in microglia. Considering the substrate specificity and involvement of PAF production, group IVA cytosolic $PLA_2$ is likely to be responsible for the increased $PLA_2$ activity. These data suggest that PAF accumulation in the SC of EAE mice is profoundly dependent on the group IVA cytosolic $PLA_2$/LysoPAFAT axis present in the infiltrating macrophages and activated microglia.** *The Journal of Immunology*, **2008, 181: 5008–5014.**

Platelet-activating factor (PAF[3]; 1-*O*-alkyl-2-acetyl-*sn*-glycero-3-phosphocholine), a potent proinflammatory lipid mediator (1), is believed to be synthesized via two distinct pathways, the de novo and remodeling pathways (Ref. 2 and see Fig. 1). The latter pathway is primarily involved in the synthesis of PAF by stimulated inflammatory cells such as murine peritoneal cells (3, 4) and human granulocytes (5). The initiation of the remodeling pathway requires membrane phospholipid hydrolysis by phospholipase $A_2$s ($PLA_2$; EC 3.1.1.4) that supply lyso-PAF, a precursor of PAF. Acetyl-CoA:lyso-PAF acetyltransferase (LysoPAFAT; EC 2.3.1.67) converts lyso-PAF into PAF. PAF activates the PAF receptor (PAFR), a member of the superfamily of G protein-coupled receptors (6), and elicits a variety of biological responses (1). PAF is rapidly degraded by PAF acetylhydrolases (PAF-AH; EC 3.1.1.47) that cleave the acetyl group at the *sn*-2 position to reform lyso-PAF (7).

$PLA_2$ are classified into three groups: group VI calcium-independent $PLA_2$s (i$PLA_2$s), secretory $PLA_2$s (s$PLA_2$s), and group IV cytosolic $PLA_2$s (c$PLA_2$) (8). Group IVA c$PLA_2$ preferentially liberates arachidonic acid from 2-arachidonoyl-phospholipids (8, 9). The released arachidonic acids are in turn converted into PGs and leukotrienes via the arachidonic acid cascade (10). It is thought that group VI i$PLA_2$ and some types of s$PLA_2$s have the potential to initiate the arachidonic acid cascade, even though these enzymes lack significant substrate specificity (8). Group IVA c$PLA_2$ is also essential for producing PAF, since PAF synthesis is significantly diminished in calcium ionophore-stimulated macrophages derived from group IVA c$PLA_2$-deficient mice as compared with those from wild-type mice (11). Recently, our group has successfully overcome the long-standing challenges of cloning and identifying LysoPAFAT (12), a critical enzyme that produces PAF. We termed the enzyme LsoPAFAT/LPCAT2 (lysophosphatidylcholine acyltransferase 2) (12). We have demonstrated that murine macrophages and neutrophils express LysoPAFAT/LPCAT2 mRNA and possess a LysoPAFAT activity (3, 12). Furthermore, LysoPAFAT/LPCAT2 mRNA is induced by the ligands for TLRs 4 and 9 in murine macrophages (12). These results imply that LysoPAFAT plays a crucial role in the enhanced PAF production in inflammatory disorders.

Multiple sclerosis (MS) is considered to be a $CD4^+$ T cell-mediated autoimmune disease and is characterized by inflammation and demyelination in the CNS (13). The mechanism of MS,

*Department of Biochemistry and Molecular Biology, Faculty of Medicine, University of Tokyo, Tokyo, Japan; and †Precursory Research for Embryonic Science and Technology of Japan Science and Technology Agency, Tokyo, Japan

Received for publication October 9, 2007. Accepted for publication July 21, 2008.

The costs of publication of this article were defrayed in part by the payment of page charges. This article must therefore be hereby marked *advertisement* in accordance with 18 U.S.C. Section 1734 solely to indicate this fact.

[1] This work was supported, in part, by Grants-in-Aid from the Ministry of Education, Science, Culture, Sports and Technology of Japan (to T. S. and S. I.), a grant to the Respiratory Failure Research Group from the Ministry of Health, Labour and Welfare, Japan (to S. I.), Grants-in-Aid for Comprehensive Research on Aging and Health from the Ministry of Health, Labour and Welfare, Japan (to S. I.), the Kato Memorial Trust for Nambyo Research (to S. I.), and the Japanese Society for the Promotion of Science (research fellowships to Y.Ki., D.H., and K.Y.). H.S., S.I., and T.S. were supported by the Center for NanoBio Integration (University of Tokyo).

[2] Address correspondence and reprint requests to Dr. Takao Shimizu, Department of Biochemistry and Molecular Biology, Faculty of Medicine, University of Tokyo, 7-3-1 Hongo, Bunkyo, Tokyo 113-0033, Japan. E-mail address: tshimizu@m.u-tokyo.ac.jp

[3] Abbreviations used in this paper: PAF, platelet-activating factor; $PLA_2$, phospholipase $A_2$; LysoPAFAT, acetyl-CoA:lyso-PAF acetyltransferase; LysoPAFAT/LPCAT2, LysoPAFAT/lysophosphatidylcholine acyltransferase 2; lyso-PAF, 1-*O*-alkyl-*sn*-glycero-3-phosphocholine; PAFR, PAF receptor; PAF-AH, PAF acetylhydrolase; PC, phosphatidylcholine; i$PLA_2$, calcium-independent $PLA_2$; s$PLA_2$, secretory $PLA_2$; c$PLA_2$, cytosolic $PLA_2$; MS, multiple sclerosis; EAE, experimental allergic encephalomyelitis; MOG, myelin oligodendrocyte glycoprotein; SC, spinal cord; ESI-MS/MS, electrospray ionization-tandem mass spectrometry; LPCAT1, lysophosphatidylcholine acyltransferase 1; APMSF, amidinophenylmethanesulfonyl fluoride; GFAP, glial fibrillary acidic protein.

however, remains obscure because of limited access to the CNS at various phases of MS. An animal model, experimental allergic encephalomyelitis (EAE), is indispensable for a better understanding of MS pathology (14). Howat et al. (15) suggested an involvement of PAF in EAE for the first time. We have found that PAFR-KO mice immunized with myelin oligodendrocyte glycoprotein (MOG) peptide 35–55 ($MOG_{35-55}$) show less severe symptoms than wild-type mice (16). Group IVA $cPLA_2$ deficiency protects mice from EAE pathology (17). We also have reported that there is a correlation between the PAF level in the spinal cord (SC) and EAE symptoms (16), which is consistent with PAF levels in the cerebrospinal fluid of relapsing-remitting MS patients (18). In the SC of EAE mice, PAF seems to exist in the nanomolar range, which is adequate to provoke biological responses through the PAFR (6). Moreover, the level of PAFR transcript is up-regulated in MS lesions (19) and the CNS of EAE-induced SJL and C57BL/6 mice (16, 20). The elevated levels of both PAF and PAFR transcripts probably worsen the MS/EAE pathology. EAE, as an animal model of MS, is useful for understanding the roles of PAF in MS (14), since studies on PAF in MS lesions are in accordance with those in EAE lesions (16, 18–20). However, the metabolic processing of PAF and involvement of LysoPAFAT/LPCAT2 in EAE pathology are largely unknown. In the present study, we have induced EAE in C57BL/6 mice with the $MOG_{35-55}$ peptide and revealed that PAF accumulation in SCs of EAE mice is dependent on the up-regulation of the expression and activities of both group IVA $cPLA_2$ and LysoPAFAT. This is the first report suggesting the involvement of LysoPAFAT/LPCAT2 in the disease models.

## Materials and Methods

### *Induction of EAE*

EAE was induced in 8-wk-old C57BL/6 female mice. The maintenance of the facility and the use of animals were in full compliance with the University of Tokyo Ethics Committee for Animal Experiments. $MOG_{35-55}$ (MEVGWYRSPFSRVVHLYRNGK), corresponding to the fragment of mouse MOG from aa 35–55, was synthesized by Sigma-Aldrich. Mice were immunized s.c. in the flank with 300 $\mu$g of $MOG_{35-55}$ peptide in 0.1 ml of PBS and 0.1 ml of CFA containing 0.4 mg of *Mycobacterium tuberculosis* (H37Ra; Difco Laboratories) on days 0 and 7 and injected i.p. with 250 ng of pertussis toxin (List Biological Laboratories) on days 0 and 2. Mice were scored as follows: 0, no sign; 0.5, mild loss of tail tone; 1.0, complete loss of tail tone; 1.5, mildly impaired righting reflex; 2.0, abnormal gait and/or impaired righting reflex; 2.5, hind limb paresis; 3.0, hind limb paralysis; 3.5, hind limb paralysis with hind body paresis; 4.0, hind and fore limb paralysis; 4.5, moribund; and 5.0, death. To understand the EAE pathology, we divided the disease course into induction, acute, and chronic phases in accordance with the clinical symptoms as previously described (Ref. 16 and Fig. 2*A*).

### *Quantification of PAF*

PAF and eicosanoid levels were estimated simultaneously as previously described (21, 22). The results of the eicosanoid levels will be published elsewhere (Y. Kihara, S. Ishii, Y. Kita, S. Uematsu, S. Akira, and T. Shimizu, unpublished data). SCs of naive mice and EAE mice were removed on days 12, 19, and 32, frozen immediately with liquid nitrogen, and stored at −80°C until use. The frozen tissues (~100 mg) were powdered with an SK-100 mill (Tokken), and lipids were extracted for 60 min at 4°C with methanol containing deuterium-labeled 16:0 PAF (Cayman Chemical) as an internal standard. The extracts were loaded onto Oasis HLB cartridges (30 mg; Waters) preloaded with methanol and 0.03% (v/v) formic acid/$H_2O$. The cartridges were washed with 0.03% formic acid/$H_2O$, 15% (v/v) ethanol, and petroleum ether. Lipids were extracted with 100% methanol and PAF levels were quantified by reversed-phase HPLC electrospray ionization (ESI)-tandem mass spectrometry (MS/MS) as described previously (21, 22).

### *Quantitative real-time PCR*

On days 11–12, 18–19, and 30–31, naive and EAE mice were anesthetized with urethane (1.5 g/kg of body; Sigma-Aldrich) and intracardially perfused with 10 ml of ice-cold PBS. The SCs were removed and total RNA was isolated using an RNeasy Mini Kit (Qiagen). The purity and integrity of total RNA were determined by the absorbance at $A_{260/280}$ and gel electrophoresis, respectively. One microgram of total RNA was reverse-transcribed using SuperScript II (Invitrogen Life Technologies) according to the manufacturer's instructions. The RT$^2$ Profiler PCR Array System for $PLA_2$ (groups IVA, IVB, IVC, IVD, IVE, and IVF $cPLA_2$s, groups V and X $sPLA_2$s, and group VI $iPLA_2$) was purchased from SuperArray, and quantitative RT-PCR for these $PLA_2$ mRNAs was performed with a 7500 Fast Real-Time PCR System (Applied Biosystems). The relative abundance of $PLA_2$ mRNA levels in EAE mice compared with naive mice was calculated by the comparative cycle threshold method using hypoxanthine phosphoribosyltransferase as a normalization control. Quantification of LysoPAFAT, lysophosphatidylcholine acyltransferase 1 (LPCAT1), and $\beta$-actin mRNA levels was performed with LightCycler FastStart DNA Master SYBR Green I (Roche) as previously described (12, 23). Results were quantified by using standard curves derived from SCs in the acute phase of EAE.

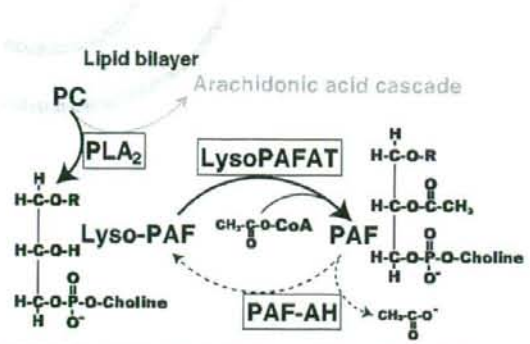


**FIGURE 1.** PAF production in the remodeling pathway (bold arrow) and degradation pathway (dotted arrow).

### *Sample preparation for enzyme assays and Western blotting*

The SCs of naive mice and EAE mice on days 12, 19, and 34 were removed following perfusion, frozen immediately with liquid nitrogen, and stored at −80°C until use. The tissues (~100 mg) were homogenized with a Physcotoron homogenizer (Microtec) in 500 $\mu$l of buffer A (100 mM Tris-HCl (pH 7.4) containing 10.26% sucrose, 20 $\mu$M amidinophenylmethanesulfonyl fluoride (APMSF), 5 mM 2-ME, and 1 × Complete Protease Inhibitor Mixture (Roche)). The homogenate was centrifuged at 9,000 × *g* for 10 min at 4°C and the resulting supernatant was centrifuged at 100,000 × *g* for 60 min at 4°C. The pellet was resuspended in buffer B (20 mM Tris-HCl (pH 7.4) containing 20 $\mu$M APMSF, 5 mM 2-ME, and EDTA-free 1 × Complete Protease Inhibitor Mixture) and stored at −80°C until use. Protein concentrations were determined by the Bradford method using a protein assay solution (Bio-Rad) and BSA (fraction V, fatty acid-free; Sigma-Aldrich) as a standard.

### *$PLA_2$ assay*

$PLA_2$ activity was measured by Dole's method with some modifications (24). Briefly, 5 $\mu$g of protein (100,000 × *g* supernatant) was incubated at 37°C for 30 min in a total volume of 0.25 ml of assay buffer (100 mM HEPES-NaOH (pH 7.4) 1 mg/ml BSA, 4 mM $CaCl_2$, and 1 mM DTT) containing mixed micelles (4 $\mu$M Triton X-100 and 2 $\mu$M 1-palmitoyl-2-[$^{14}$C]arachidonoyl-phosphatidylcholine (PC) (1.961 GBq/mmol, GE Healthcare BioSciences). The reaction was terminated by adding 1.25 ml of Dole's reagent (isopropanol:*n*-heptane:sulfuric acid, 78:20:2), followed by the sequential addition of 0.75 ml of *n*-heptane and 0.5 ml of water. After centrifugation, an aliquot (0.8 ml) of the upper layer was mixed with 120–150 mg of silica gel, which had been preincubated with 0.75 ml of *n*-heptane. The radioactivity of an aliquot (0.8 ml) was estimated using an LS6500 liquid scintillation counter (Beckman Coulter) in the presence of 1 ml of Microscinti-0 (PerkinElmer).

### *LysoPAFAT assay*

LysoPAFAT activity was measured according to the method of Kume et al. (4, 12, 25), with some modifications. Briefly, 5 $\mu$g of protein (100,000 ×

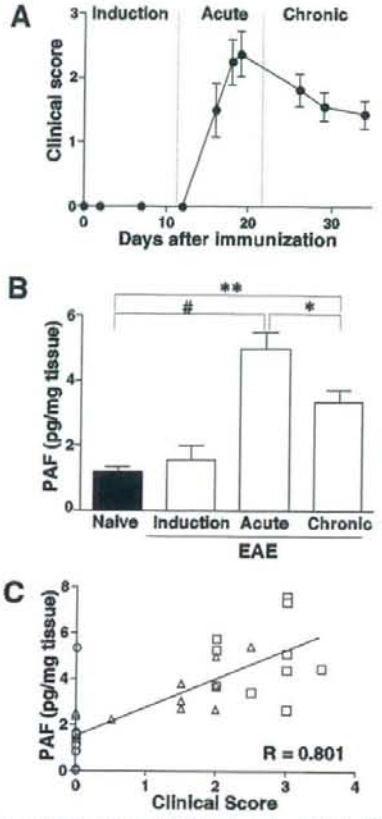


FIGURE 2. Clinical course and PAF levels during EAE. *A*, C57BL/6 female mice were immunized with the $MOG_{35-55}$ peptide. Data are the mean clinical scores ± SEM of eight animals. *B*, PAF levels were determined in SCs of naive mice and EAE mice in the induction, acute, and chronic phases ($n$ = 10 animals). Data represent means ± SEM. #, $p < 0.001$; **, $p < 0.01$; and *, $p < 0.05$ by ANOVA with the Tukey-Kramer test. *C*, PAF levels of naive (●) and EAE mice in the induction (○), acute (□), and chronic (△) phases are positively correlated with the clinical scores ($p < 0.0001$ by the Spearman rank correlation test). Each data point represents the result from a single animal.

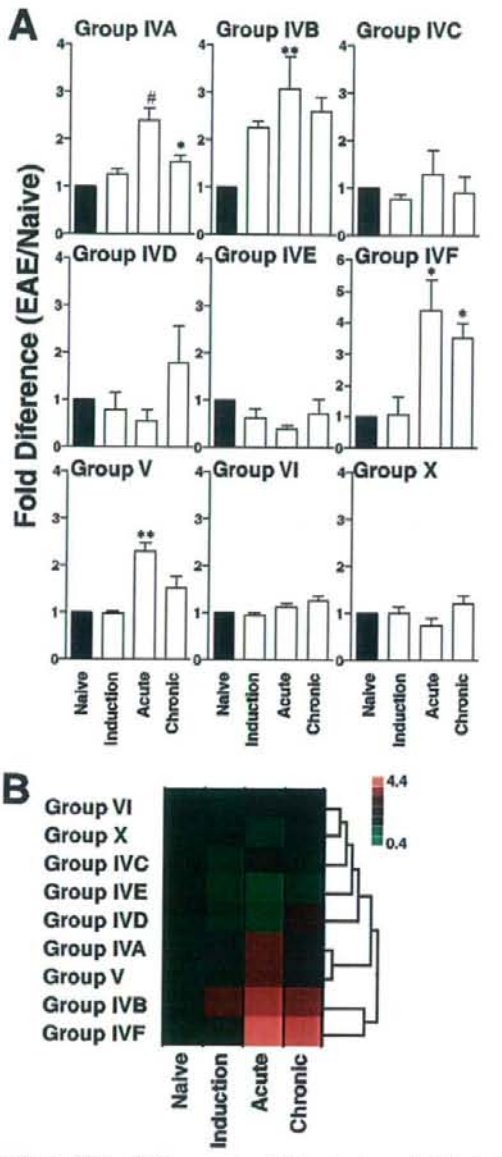


FIGURE 3. $PLA_2$ mRNA expression in SCs of naive and EAE mice. *A*, Expression of $PLA_2$ transcripts was quantified by real-time PCR in SCs of naive mice and EAE mice in the induction, acute, and chronic phases ($n$ = 6, 5, 6, and 5 animals, respectively). The relative abundance of $PLA_2$ mRNA levels in EAE mice compared with naive mice is shown. Data represent means ± SEM. #, $p < 0.001$; **, $p < 0.01$; and *, $p < 0.05$ compared with naive mice by the Kruskal-Wallis test with Dunn's post hoc test. *B*, The relationships among $PLA_2$ mRNA levels were evaluated by cluster analysis using JMP6 software (Hulinks). The relative expression levels shown in *A* are divided into seven parts and colored from red to green.

$g$ pellet) was incubated at 37°C for 10 min in a total volume of 0.1 ml of reaction mixture (buffer B containing 2 mM $CaCl_2$, 1 mg/ml PC (Sigma-Aldrich), and 100 $\mu$M [$^3$H]acetyl-CoA (1.11 GBq/mmol; GE Healthcare BioSciences)) with or without 20 $\mu$M lyso-PAF (Cayman Chemical). Subsequently, 122 $\mu$l of ice-cold methanol was added to terminate the reaction. The product was bound to 6 mg of C8 resin (Millipore), washed eight times with 55% (v/v) methanol in 20 mM Tris-HCl (pH 7.4), and eluted with 100% methanol. After drying at 50°C for 2 h, the radioactivity was determined using a TopCount microplate scintillation counter (PerkinElmer) in the presence of 200 $\mu$l of Microscinti-0. LysoPAFAT activity was calculated by subtracting the radioactivity obtained without lyso-PAF from that obtained with lyso-PAF.

*PAF-AH assay*

PAF-AH activity was evaluated under the same conditions as reported previously, with minor modifications (26, 27). Briefly, 10 $\mu$g of protein (100,000 × $g$ supernatant) was incubated at 37 °C for 30 min in a total volume of 0.25 ml of assay buffer (50 mM Tris-HCl (pH 7.4), 5 mM EDTA, 5 mM 2-ME, and 100 $\mu$M [*acetyl*-$^3$H]PAF (85 MBq/mmol; PerkinElmer)). The reaction was stopped by adding 2.5 ml of chloroform/methanol (4:1, v/v), followed by 0.25 ml of water. The radioactivity of an aliquot (0.6 ml) of each water phase was measured with 2 ml of the liquid scintillation mixture, Atomlight (PerkinElmer), to determine the amount of acetyl groups liberated from PAF.